The visual white matter: The application of diffusion MRI and fiber tractography to vision science

Ariel Rokem[1], Hiromasa Takemura[2], Andrew Bock[3], K. Suzanne Scherf[4], Marlene Behrmann[5], Brian Wandell[6], Ione Fine[7], Holly Bridge[8], and Franco, Pestilli[9]

[1]The University of Washington eScience Institute, Seattle, WA, USA, http://arokem.org, arokem@uw.edu
[2]Center for Information and Neural Networks (CiNet), National Institute of Information and Communications Technology, Graduate School of Frontier Biosciences, Osaka University, Suita, Japan
[3]University of Pennsylvania, Phildelphia, PA, USA
[4]Penn State University, State College, PA, USA
[5]Carnegie Mellon University, Pittsburgh, PA, USA
[6]Stanford University, Stanford, CA, USA
[7]University of Washington, Seattle, WA, USA
[8]Oxford University
[9]University of Indiana, Bloomington, IN, USA, http://pestillilab.indiana.edu, franpest@indiana.edu

Keywords: MRI, diffusion MRI, brain, white matter, brain connectivity, visual cortex, visual disability, visual development, categorical perception, face perception, software, computational modeling.

Abstract

Visual neuroscience has traditionally focused much of its attention on understanding the response properties of single neurons or neuronal ensembles. The visual white matter and the long-range neuronal connections it supports is fundamental in establishing such neuronal response properties as well as visual function. This review article provides an introduction to measurements and methods to study the human visual white matter using diffusion MRI (dMRI). These methods allow us to measure the white matter micro- and macro-structural properties in living human individuals; they allows us to trace long-range connections between neurons in different parts of the visual system, and to measure the biophysical properties of these connections. We also review a range of findings from recent studies on connections between different visual field maps, on the effects of visual impairment on the white matter, and on the properties underlying networks that process visual information that supports visual face recognition. Finally, we discuss a few promising directions for future studies. These include new methods for analysis of MRI data, open data-sets that are becoming available to study brain connectivity and white matter properties, and open-source software for the analysis of these data.

1 Introduction

The cerebral hemispheres of the human brain can be subdivided into two primary tissue types: the white matter and the gray matter (Fields, 2008a). Whereas the gray matter contains neuronal cell bodies, the white matter contains primarily the axons of these neurons, and glial cells. The axons constitute the connections that transmit information between distal parts of the brain - mm to cm in length. Some types of glia (primarily oligodendrocytes) form an insulating layer around these axons (myelin sheaths) that allow the axons to transmit information more rapidly (Waxman and Bennett, 1972), and more accurately (Kim et al., 2013), and reduce their energy consumption (Hartline and Colman, 2007).

Much of neuroscience has historically focused on understanding the functional response properties of individual neurons and cortical regions (Fields, 2013, 2004). It has often been implicitly assumed that white matter, and the long-range neuronal connections it supports have a binary nature: either they are connected and functioning, or they are disconnected. However, more recently there is an increasing focus on the role that the variety of properties of the white matter may play in neural computation (Bullock et al., 2005; Jbabdi et al., 2015; Reid, 2012; Sporns et al., 2005) together with a growing understanding of the importance of the brain networks composed of these connections in cognitive function (Petersen and Sporns, 2015).

The renewed interest in white matter is in part due to the introduction of new technologies. Long-range connectivity between parts of the brain can be measured in a variety of ways. For example, functional magnetic resonance imaging (fMRI) is used to measure correlations between the blood-oxygenation level dependent (BOLD) signal in different parts of the brain. In this review, we focus on results from diffusion-weighted Magnetic Resonance Imaging technology (dMRI). Together with computational tractography dMRI provides the first opportunity to measure white matter and the properties of long-range connections in the living human brain. We will refer to these connections as “fascicles”, an anatomical term that refers to bundles of nerve or muscle. Measurements in living brains demonstrate the importance of white-matter for human behavior, health and disease (Fields, 2008a; Jbabdi et al., 2015; Johansen-Berg and Behrens, 2009) development (Lebel et al., 2012; Yeatman et al., 2014a) and learning (Bengtsson et al., 2005; Blumenfeld-Katzir et al., 2011; Hofstetter et al., 2013; Sagi et al., 2012; Sampaio-Baptista et al., 2013; Thomas and Baker, 2013). The white matter comprises a set of active fascicles that respond to human behavior, in health and disease by adapting their density, their shape, and their molecular composition and correspond to human cognitive, motor and perceptual abilities.

The visual white matter sustains visual function. In the primary visual pathways, action potentials travel from the retina via the optic nerve, partially cross at the optic chiasm, and continue via the optic tract to the lateral geniculate nucleus (LGN) of the thalamus. From the LGN, axons carry visual information laterally through the temporal lobe, forming the structure known as Meyer’s loop, and continue to the primary visual cortex (Figure 1). The length of axons from the retina to the LGN is approximately 5 cm long, while the length of the optic radiation from the anterior tip of Meyer’s loop to the calcarine sulcus is approximately 10 cm, with an approximate width of 2 cm at the lateral horn of the ventricles (Peltier et al., 2006; Sherbondy et al., 2008b). Despite traveling the entire length of the brain, responses to visual stimuli in cortex arise very rapidly (Maunsell and Gibson, 1992), owing to the high degree of myelination of the axons in the primary visual pathways. Healthy white matter is of crucial importance in these pathways, as fast and reliable communication of visual input is fundamental for healthy visual function

This review presents the state of the art in dMRI studies of the human visual system. We start with an introduction of the measurements and the analysis methods. Following that, we review three major applications of dMRI:

1. The delineation of the relationship between visual field maps and the white matter connections between the maps. This section focuses on a test-case of the connections between dorsal and ventral visual field maps.

2. The effects of disorders of the visual system on the visual white matter. This section focuses on the changes that occur in the white matter in cases of peripheral and cortical blindness, and on white matter connectivity that underlies cross-modal plasticity and residual vision respectively in these cases.

3. The role that the visual white matter plays in visual discrimination of specific categories of visual objects. In particular, this section focuses on the white matter substrates of the perception of face stimuli.

Taken together, these three sections present multiple facets of dMRI research in vision science, covering a wide array of approaches and applications. They all demonstrate the ways in which studying the white matter leads to a more complete understanding of the biology of the visual system: its structure, response properties and relation to perception and behavior. In the summary of the review we will point out some common threads among these applications, point to a few of the challenges facing the field, and the promise of future developments to help address some of these challenges.

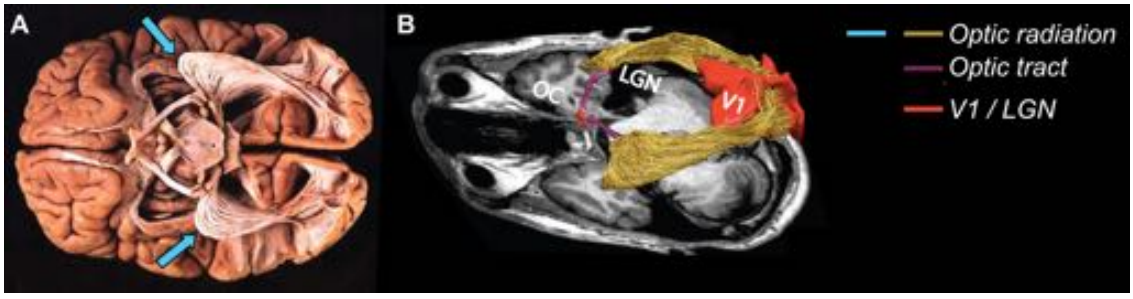

Figure 1: Postmortem and in vivo study of the visual white matter. **A**. Post mortem dissection of the optic radiation (OR), showing the Meyer's loop bilaterally (blue arrows; adapted from (Sherbondy et al., 2008b). **B**. In vivo dissection of the optic radiation showing the optic chiasm (OC), Meyer's loop, the optic tract as well as both primary visual cortex (V1) and the lateral geniculate nucleus (LGN; (Ogawa et al., 2014))

Methods for in-vivo study of the human white matter

In this section, we introduce concepts and methods for measuring white matter connections using dMRI. The text is accompanied by a series of code examples implemented as Jupyter notebooks, which can be downloaded from `https://github.com/arokem/visual-white-matter`.

Measuring white matter using diffusion magnetic resonance imaging

Diffusion MRI measures the directional diffusion of water in different locations in the brain. In MRI, a strong magnetic field is applied to the brain, causing protons in water molecules to precess at a field-strength-dependent frequency. When the magnitude of the magnetic field is varied linearly in space (creating a a magnetic field gradient), protons in different locations along the gradient begin

to precess at different rates. The rate of precession varies spatially along the same direction as the magnetic gradient. Diffusion MRI utilizes a second gradient pulse with the same magnitude but in the opposite direction that refocuses the signal by aligning the spins of water molecules. Refocusing will not be perfect for protons that have moved during the time interval between the gradient pulses, and the resulting loss of signal from dephasing is used to infer the mean diffusion of water molecules (due to random Brownian motion) along the direction of the magnetic gradient. Measurements conducted with gradients applied along different axes sensitize the signal to diffusion in different directions (Figure 1B).

Additional magnetic field gradients are used to render the measurements spatially selective. In-vivo measurements in human typically use resolutions on the order of 2x2x2 mm^3 (isotropic voxels). Using modern imaging techniques, such as multi-band imaging (Feinberg et al., 2010), high SNR measurements can be done in vivo with voxel sizes as small as 1.25-1.5 mm (isotropic) (Setsompop et al., 2013) using standard 3 Tesla (3T) hardware. Post-mortem and animal measurements can be done with much smaller size scale, down to approximately 200 μm (isotropic) (Leuze et al., 2014; Reveley et al., 2015).

The sensitivity of the measurement to diffusion increases with the amplitude and duration of the magnetic field gradient, as well as with the time between the two gradient pulses (the *diffusion time* or *mixing time*). These three parameters are usually summarized in a single number: the b-value (see code example: `http://arokem.github.io/visual-white-matter/signal-formation`). Increased diffusion-sensitivity does come at a cost: measurements at higher b-values also have lower SNR. In the typical dMRI experiment, diffusion times are on the order of 50-100 $msec$. Within this time-scale, at body temperature, water molecules may diffuse an average of approximately 20 μm, when no restriction is placed on their diffusion (at body temperature) (Le Bihan and Iima, 2015). This rate of diffusion is found in the ventricles of the brain, for example. Within other brain structures the average diffusion distance is impeded by the brain tissue (Figure 1; see also: `http://arokem.github.io/visual-white-matter/dMRI-signals`).

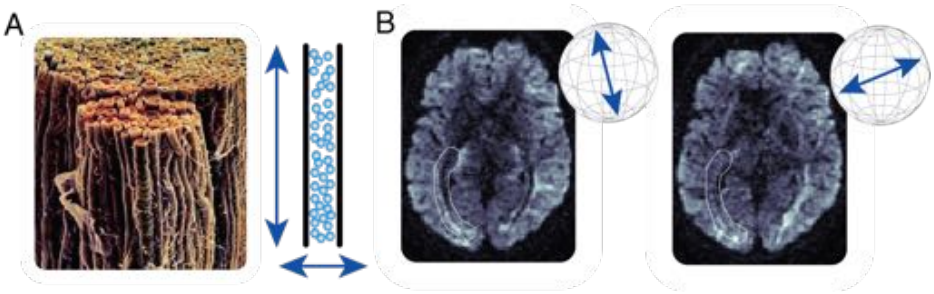

Figure 2: Inferences about white matter from measurements of water diffusion. A Micrograph of the human optic nerve. Left, bundles of myelinated axonal fascicles from the human optic nerve (image courtesy of Dr. George Bartzokis). Right, cartoon example of anisotropic water diffusion restriction by white matter fascicles . Water diffuses further along the direction of the "tube" (Pierpaoli and Basser, 1996). **B** Example of diffusion-weighted magnetic resonance measurements in a single slice of a living human brain. The same brain slice is shown as imaged with two different diffusion weighting directions. Diffusion weighting directions are shown by the inset arrows. The white highlighted area indicates the approximate location of part of the OR. The longitudinal shape of the OR appears as a local darkening of the MRI image when the diffusion weighting gradient is aligned with the direction of the myelinated fascicles within the OR, right-hand panel

In regions of the brain or body that contain primarily spherically-shaped cell bodies, water diffusion is equally restricted in all directions: it is isotropic. On the other hand, in fibrous biological structures, such as muscle or nerve fascicles, the diffusion of water is restricted across the fascicles (e.g. across axonal membranes) more than along the length of the fascicles (e.g. within the axoplasm). In these locations, diffusion is anisotropic. Measurements of isotropic and anisotropic diffusion can be used to estimate the microstructural properties of brain tissue and brain connectivity.

Inferring brain tissue properties and connectivity from dMRI data generally involves two stages: the first estimates the microstructure of the tissue locally in every voxel. The second stage connects local estimates across voxels to create a macrostructural model of the axonal pathways. We review approaches to these two stages in the sections that follow.

Estimating brain microstructure: models of diffusion in single voxels

Even though diffusion MRI samples the brain using voxels at millimeter resolution, the measurement is sensitive to diffusion of water within these voxels at the scale of μm. This makes dMRI a potent probe of the aggregate microstructure of the brain tissue in each voxel. A variety of analytic techniques and different models are routinely used to model tissue microstructure in brain voxel. We present two of the major approaches below.

The diffusion tensor model

The diffusion tensor model (DTM; (Basser et al., 1994a,b); see: `http://arokem.github.io/visual-white-matter/dtm`) approximates the directional profile of water diffusion in each voxel as a 3D Gaussian distribution. The direction in which this distribution has its largest variance is an estimate of the principal diffusion direction (PDD; Figure 3) – the direction of maximal diffusion. In many places in the brain, the PDD is aligned with the orientation of the main population of nerve fascicles and can be used as a cue for tractography (see below). In addition to the PDD, the diffusion tensor model provides other statistics of diffusion: the mean diffusivity (MD), which is an estimate of the average diffusivity in all directions, and the fractional anisotropy (FA), which is an estimate of the variance in diffusion in different direction (Pierpaoli and Basser, 1996) (Figure 3). These statistics are useful for characterizing the properties of white matter and numerous studies have shown that variance in these statistics within relevant white matter tracts can predict individual differences in perception (Genç et al., 2011), behavioral and cognitive abilities (e.g. (Yeatman et al., 2011), and mental health (Thomason and Thompson, 2011). A major advantage of the DTM is that it can be estimated from relatively few measurement directions: accurate (Rokem et al., 2015) and reliable (Jones, 2004) estimates of the tensor parameters require measurements in approximately 30-40 directions, which requires approximately 10 minutes for a full-brain scan in a clinical scanner.

The interpretation of tensor-derived statistics is not straight-forward. MD has been shown to be sensitive to the effects of stroke during its acute phases (Mukherjee, 2005), and loss of nerve fascicles due to Wallerian degeneration and demyelination also results in a decrease in FA (Beaulieu et al., 1996). These changes presumably occur because of the loss of density in brain tissue. The decrease in FA can be traced directly to the loss of myelin structure, which allows for more diffusion of extra-cellular water. But FA also decreases in voxels in which there are crossing fascicles (Pierpaoli and Basser, 1996; Frank, 2001, 2002), rendering changes in FA ambiguous. A recent study estimated that approximately 90% of the white matter contains crossings of multiple fascicles populations (Jeurissen et al., 2013). Therefore, it is unwarranted to infer purely from high

FA measures of myelination or in some individuals that these individuals have higher "white matter integrity" (Jones et al., 2013).

In an analogous issue, in voxels with crossing fascicles, the PDD will report the weighted average of the individual fascicles directions, rather than the direction of any one of the fascicles (Rokem et al., 2015). These issues have led to increasing interest in models that represent multiple fascicles within a voxel. Nevertheless, despite its limitations, the statistics derived from the diffusion tensor model provide useful information about tissue microstructure. This model has been so influential that "Diffusion Tensor Imaging" or "DTI" is often used as a synonym for dMRI.

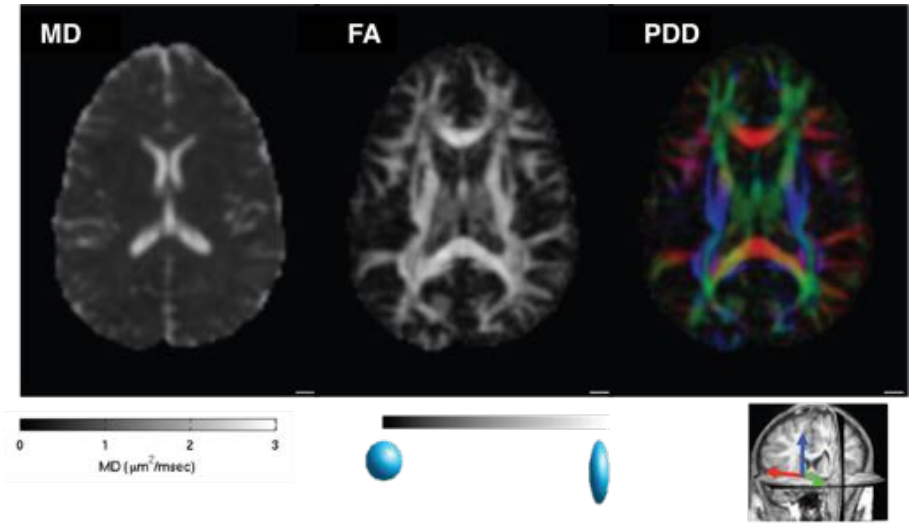

Figure 3: Diffusion tensor imaging The figure shows the three primary estimates of white matter organization derived from the diffusion tensor model measured in a single slice of a human brain (spatial resolution = 2 mm^3, b-value = 900 s/mm^2). **Mean diffusivity**(MD, left) represents water diffusion averaged across all measured diffusion direction. The value is expected to be 3 $\mu m^2/msec$ for pure water (in body temperature) and indeeed, MD is close to 3 in the ventricles. **Fractional anisotropy** (FA, middle) represents the variability of diffusion in different directions. This value is unit-less, and bounded between 0 and 1 and it is highest in voxels containing a single dense fascicle, such as in the corpus callosum. The **principal diffusion direction**(PDD, right) is the direction of maximal diffusion in each voxel. It is often coded with a mapping of the X,Y and Z components of the direction vector mapped to R,G and B color channels respectively, and scaled by FA. Main white matter structures such as the corpus callosum (red, along the right-to-left x axis) and the corticospinal tract (blue, along the superior-inferior y axis) are easily detected in these maps.

Crossing fiber models

One limitation of the diffusion tensor model that was recognized early on (Pierpaoli and Basser, 1996) is that it can only represent a single principal direction of diffusion. Starting with the work of Larry Frank (Frank, 2001, 2002), there have been a series of models that approximate the dMRI signal in each voxel as a mixture combined from the signals associated with different fascicles within each voxel (Tournier et al., 2004; Behrens et al., 2007; Dell'Acqua et al., 2007; Tournier et al., 2007; Rokem et al., 2015)

(see code example: `http://arokem.github.io/visual-white-matter/SFM`). Common to all

these models is that they estimate a fascicle orientation distribution function (fODF), based on the partial volumes of the different fascicles contributing to the mixture of signals. These models are more accurate than the diffusion tensor model in regions of the brain where large populations of nerve fascicles are known to intersect, and also around the optic radiations (Figure 4) (Alexander et al., 2002; Rokem et al., 2015)

A second approach to modeling complex configurations of axons in a voxel are offered by so-called "model free" analysis methods, such as q-space imaging (Tuch, 2004) and diffusion spectrum imaging (DSI; (Wedeen et al., 2005)). These analysis methods estimate the distribution of orientations directly from the measurement, using the mathematical relationship between the dMRI measurement and the distribution of diffusion in different directions, and without interposing a model of the effect of individual fascicles and the combination of fascicles on the measurement. These approaches typically require a larger number of measurements in many diffusion directions and diffusion weightings (b-values), demanding a long measurement duration.

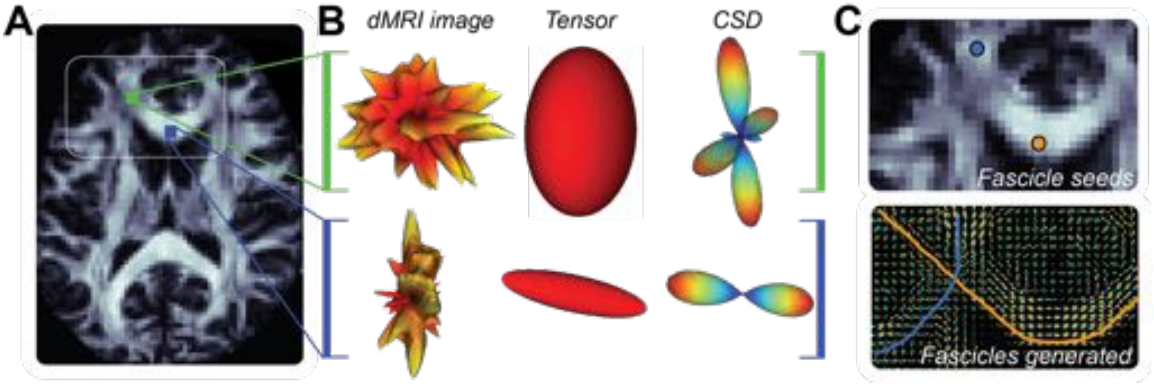

Figure 4: Relation between diffusion MRI signals, voxel models of diffusion and tractography **A** An axial brain slice. Two voxels locations are indicated in blue and green. The white rectangle indicates the location of the images in **C**. **B** Measured diffusion-weighted MR image in the colored locations in A. Left column. Diffusion signal for the green (top) and blue (bottom) locations rendered as 3D surfaces, with the color map indicating the intensity of the diffusion-weighted signal in each direction (red is low signal or high diffusion and yellow-white is high signal, or low diffusion). *Middle column*: The three-dimensional Gaussian distribution of diffusion distance, estimated from the DTM for the signal to the left. The major axis of the ellipsoid indicates the principal diffusion direction estimated by the tensor model, different for the two voxels. *Right column*: Fascicle orientation distribution function (fODF) estimated by a fascicle mixture model: the constrained spherical deconvolution (CSD) model (Tournier et al., 2007) from the signal to its left. CSD indicates several probable directions of fascicles. Colormap indicates likelihood of the presence of fascicles in a direction. **C** *Top panel*: Detail of the region highlighted in **A** (white frame) with example of two seeds randomly placed within the white matter and used to generate the fascicles in the bottom panel. *Bottom panel*: Fits of the CSD model to each voxel and two example tracks (streamlines) crossing at the location of the centrum semiovale.

Estimating white matter macrostructure: methods for tracking long-range brain fascicles and connections.

Computational tractography refers to a collection of methods designed to make inferences about the macroscopic structure of white matter pathways (Figure 5C; (Jbabdi et al., 2015): these al-

gorithms combine models of the local distribution of neuronal fascicles orientation across multiple voxels, to "track" long-range neuronal pathways. These pathways are generally interpreted as aggregated neuronal projections fascicles, rather than individual axons: brain "highways" that connect distal brain areas, that are millimeters to centimeters apart. Below we describe tractography by dividing it into three major phases of analysis: initiation, propagation, and termination of tracking.

Track initiation

The process of tractography generally starts by seeding a certain arbitrary number of fascicles within the white matter tissue identified by methods for tissue segmentation (Fischl, 2012). Tracking is generally initiated in many locations within the white matter volume. In several cases, fascicles are seeded within spatially constrained regions of interest. This is the case when the goal is to identify brain connections by tracking between two specific brain areas (Smith et al., 2012).

Track propagation

Three major classes of algorithms are used to propagate tracks: deterministic, probabilistic and global. *Deterministic tractography* methods take the fascicles directions estimated in each voxel at face value and draw a streamline by following the principal fascicle directions identified by the voxel-wise model fODF (see above and `http://arokem.github.io/visual-white-matter/det_track`).

Probabilistic tractography methods (Conturo et al., 1999; Mori et al., 1999; Mori and Van Zijl, 2002; Behrens et al., 2003, 2007; Tournier et al., 2012)) accept the voxel-wise estimate of the fODF, but recognize that such estimates may come with errors. Instead of strictly following the directions indicated by the fODF, they consider the fODF to be a probability distribution of possible tracking directions. These methods generate tracks aligned with the principal fiber directions, with higher probability, but they also generate tracks away from the principal directions with non-zero probability (code example: `http://arokem.github.io/visual-white-matter/prob_track`). *Global tractography* methods build streamlines that conform to specified 'global' properties or heuristics (Mangin et al., 2013; Reisert et al., 2011). For example, some algorithms constrain streamlines to be spatially smooth (Aganj et al., 2011).

Track termination

Tractography is generally restricted to the white matter volume, so when tracks reach the end of the white matter they are terminated. To determine the extent of the white matter, we can rely on: methods of tissue segmentation based on anatomical measurements (Fischl, 2012) (see `http://arokem.github.io/visual-white-matter/det_track` for an example) or differences in diffusion properties between different tissue types. For example, because gray matter has low FA, tracking is often terminated when FA drops below a specific threshold (historically FA values of 0.2 or 0.1 have been used as tracking stopping thresholds).

The Fascicle Detection Problem

Computational fascicle estimated using tractography should be considered as putative models of the structure of neuronal fascicles. Tractography can and does make mistakes and we are far from obtaining gold standard estimates of white matter anatomy and connections using these

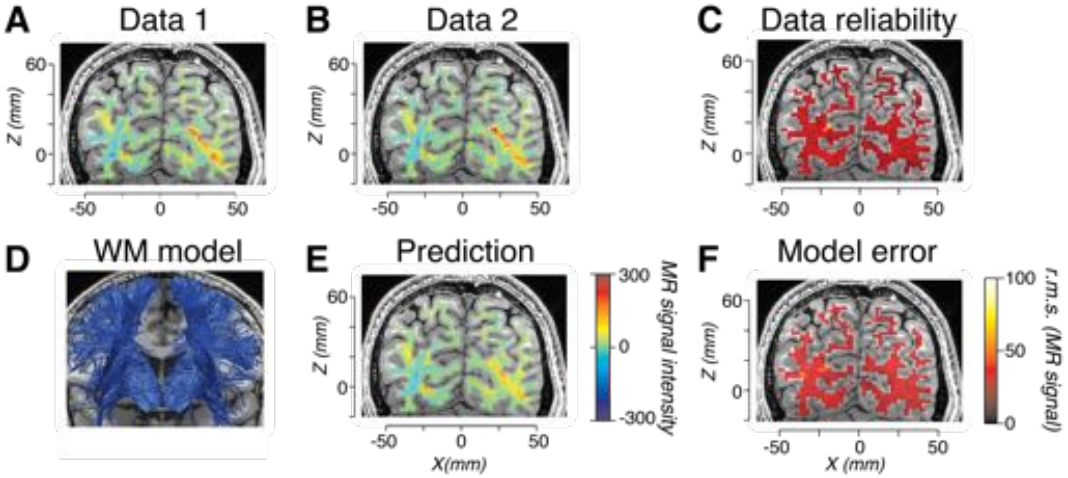

Figure 5: Models of white matter anatomy and tractography evaluation. **A** Measurement of a single diffusion direction shown on a coronal slice of a living human brain. **B**. Repeated measurement of the same direction in **A**, collected during the same scanning session, using the same scanner, sequence, and subject. **C** The reliability of the data, the root mean difference comparing Data 1 and 2 expressed by the color map. **D**. Portion of a full-brain connectome model, comprising part of the corona radiata. Fascicles estimated using Data 1 (**B**) and CSD-based probabilistic tractography. E. Predicted anisotropic diffusion from the model in D, diffusion direction shown is the same as in A and B. Diffusion prediction obtained using the linear fascicle evaluation method, LiFE (Pestilli et al., 2014). **F**. Connectome model accuracy. Root mean-squared error between Data 2 and the model prediction (**E**). Modified from (Pestilli et al., 2014).

computational methods. To date, we know that we can validly identify major white matter tracts (Wakana et al., 2007; Yeatman et al., 2012). Yet the fundamental and fine properties of the white matter anatomy are still unknown and matter of debate (for example see (Wedeen et al., 2012a; Catani et al., 2012; Wedeen et al., 2012b)). There is a difficulty in the field in the ability to validate white matter models. Ideally, tractography would be validated routinely in each individual (on a case-by-case basis; Pestilli et al. (2014); Pestilli and Franco (2015)). In the absence of the needed methods several approaches have been proposed to tractography validation.

Post-mortem validation methods have been proposed to show the degree to which tractography can and cannot identify connections found by tracing and histological methods. Unfortunately, such approach cannot contribute to in-vivo understanding of brain function and disease progression. Furthermore, even if multiple brains were to be available for direct inspection with histological and anatomical methods, validation would be difficult as histological validation methods have their own limitations (Goga and Türe, 2015; Simmons and Swanson, 2009; Bastiani and Roebroeck, 2015). Thus, while the ability of most methods to identify major tracts has been validated, it remains difficult to determine whether estimates of tract differences within groups or individuals as measured using dMRI genuinely and accurately correspond to anatomical differences. This has led to interest in more direct methods of validation, such as validation with phantoms of known structure or with simulations (Côté et al., 2013).

Recently, methods that directly estimate the error of a tracking method with respect to the MRI data have been proposed (Daducci et al., 2015; Pestilli et al., 2014; Sherbondy et al., 2008a; Smith et al., 2015). These methods all rely on a forward model approach: the estimated tracts are used to generate a synthetic version of the measured diffusion signal and to compute the tractogra-

phy model error, by evaluating whether the synthetic and measured data match each other (Figure 5; code example: `http://arokem.github.io/visual-white-matter/fascicle-evaluation`). These methods allow evaluation of tractography but not necessarily validation of the anatomy of the final results (Daducci et al., 2016).

Relating tractography estimates to brain structures can be conceptualized within the established signal detection theory framework (Green and Swets, 1966). The primary goal of tractography is to detect white matter fascicles and connections. Figure 6 shows the conceptualization of tractography as a signal detection process: every time we track in a brain, there are three potential outcomes of the process; it can identify incorrect fascicles (false alarm), it can miss real fascicles (miss) or it can identify correct white matter fascicles (hits). We call this the *fascicle detection problem* or FDP.

Deterministic and probabilistic methods introduced above, use different criteria for the FDP. Deterministic tractography uses a conservative criteria, where it is assumed that each voxel contains only one or few fascicles. The false alarm rate is lower but the miss rate is also higher. The hit rate may also be low, if the fODF used in each voxel does not properly describe the biology of the white matter. Probabilistic tractography uses a more liberal criterion because fascicles can be created using the full extent of the fODF in each voxel. These methods create a higher number of false alarms, but are also more likely to generate hit fascicles (i.e., identify existing fascicles; see also Cote et al. (Côté et al., 2013) for a classification of tractography errors). Global tractography methods lie somewhere between deterministic and probabilistic methods. Their position in the continuum between the very conservative deterministic methods and the very liberal probabilistic methods depends on the details of the global tractography algorithm.

The process of fascicle detection is akin to signal interpretation processes in many other scientific fields where data resolution and signal-to-noise ratio (SNR) limit what can be measured and where methods for data analysis limit how well the signals in the data can be exploited to make inferences. Diffusion data resolution (both angular, the number of diffusion directions measured and spatial resolution, the size of the voxels) and tractography methods (probabilistic vs. deterministic, for example) can change the configuration of fascicles that can be detected. Major white matter tracts can be detected using lower-resolution data. Smaller fascicles might require higher resolution data (Vu et al., 2015). For example, because the the white matter around visual cortex is thin and convoluted, lower resolution dMRI data fails to provide information about connections between the two (dorsal and ventral) banks of the calcarine sulcus. Changing the spatial resolution of the data (e.g., by using a ultra high-field scanner) allows the same tractography methods to find connections between the dorsal and ventral calcarine sulcus (Figure 6B). At the same time, for a given data-set (with its spatial and angular resolution, and SNR) changing tractography methods can change the white matter pathways that are identified. For example, Fig. 6C (left) shows how a “u-fiber” system connecting between human dorsal V3A and V3 can be missed when a conservative curvature parameter is used in probabilistic tractography. Changing the parameters of curvature allows detection of short “u-fibers”, such as the one in Fig. 6C (right). Changing the resolution of the data (number of measured diffusion directions or spatial resolution) is akin to changing d’ (Fig. 6A): increased data resolution improves the sensitivity of the diffusion data, disambiguating signals generated by complex fascicle configurations. Changes in tractography method or parameters may reduce the missed fascicles or the false alarms, but it does not speak to increased sensitivity in detection of white matter pathways. The dilemma is that the best analysis method is likely to depend on the properties of the data as well as the fascicle to be estimated.

A recently-proposed procedure combines the best characteristics of fascicles generated by multiple tractography algorithms (Takemura et al., 2016). The method, called Ensemble Trac-

tography, generates multiple tractography solutions, based on different tractography algorithms. Fascicle evaluation (Pestilli et al., 2014) is then used to arbitrate between the different solutions provided by the different algorithm settings, allowing the method to capitalize on several different levels of sensitivity, while maintaining an accurate representation of the measured signal. Figure 6C shows that this method identifies complex fascicles configurations, easily missed by a single tractography method.

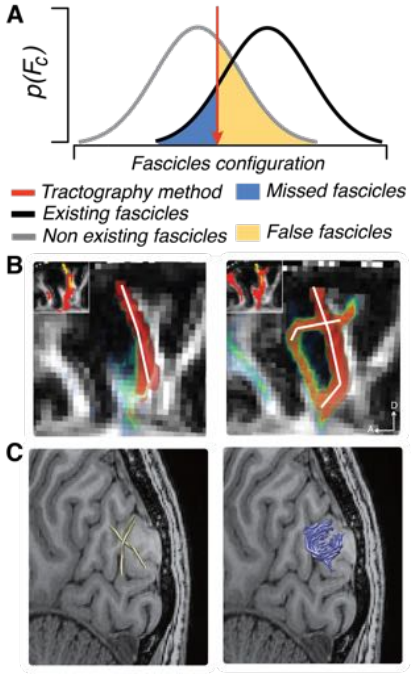

Figure 6: Identifying white matter tract and the signal detection process..A The process of tractography described using Signal Detection Theory. The brain contains a certain number of true fascicles (black). The resolution of the diffusion data (either spatial or directional resolution) can provide ambiguous signals indicating fascicles configurations for both existing (black) and non-existing fascicles configurations (gray). Tracking algorithms allow identifying some existing fascicles (right-hand side of the red criterion line), but can miss others (blue highlight), and sometimes can track non-existing fascicles (yellow). **B**. Example of increasing sensitivity for detecting complex fascicles configurations. Left, lower resolution data (1.25 mm^3). Right, higher resolution data (0.7 mm^3). Increasing data resolution improves fascicles detection. This process is akin to changing d' in the distributions in **A**. **C** Given a fixed data resolution (1.5 mm3 in the example); (Takemura et al., 2016)) changing tractography methods can allow detecting more fascicles, this is akin to a change in criterion in A. In the figure whereas using a conservative turning radius (2 mm) for the streamlines being generated does not allow capturing short-range u-fiber systems (green), using more liberal turning radius (0.5 mm) allows capturing fine details of the anatomy such as short range u-fibers (blue)

Comparing tracks and connections across individuals

Once white matter tracts and brain connections have been identified using tractography these estimates have traditionally been analyzed in three ways:

1. Identify major white matter pathways (Catani and Thiebaut de Schotten, 2008; Catani et al., 2002). One typical step after tractography is to cluster these curves together into groups (Garyfallidis et al., 2012; Wassermann et al., 2010) align these curves to each other, either across different individuals, or across hemispheres (Garyfallidis et al., 2015), or to standard anatomical landmarks (Wakana et al., 2007; Yeatman et al., 2012; Yendiki et al., 2011). For example, the optic radiation (Kammen et al., 2015; Sherbondy et al., 2008b) and other connections between thalamus and visual cortex (Ajina et al., 2015; Allen et al., 2015) can systematically be identified in different individuals based on their end-points.

2. Estimate micros-tructural tissue properties (such as FA and MD) within white matter tracts (Yeatman et al., 2012; Yendiki et al., 2011) (see Figure 7 A and B).

3. Estimate connectivity between different regions of the cortex (Jbabdi et al., 2015; Rubinov et al., 2009)(See Figure 7C).

All these estimates are combined across individuals and either groups of individuals are compared for statistical significance (for examples by comparing patient groups to control groups) or the estimates are correlated with phenotypic properties and behavior to find correlations between white matter properties and other aspects of human health and behavior of interest. Below we present multiple cases of how such group analyses have been applied to study visual function.

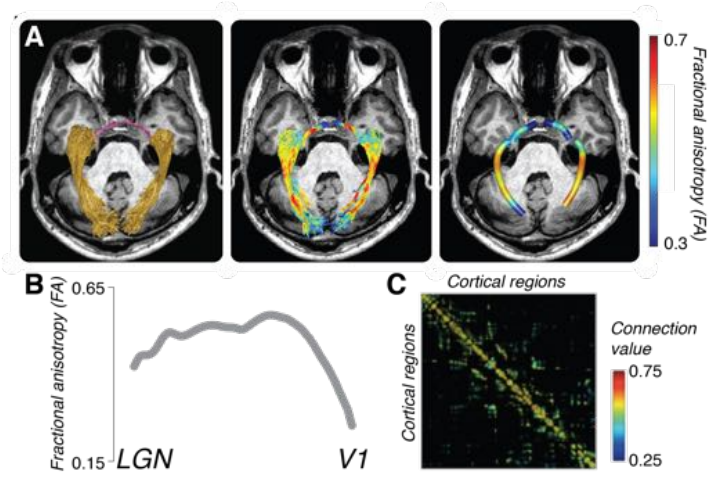

Figure 7: Example applications of tractography to study brain connections and white matter **A** Estimates of the optic radiation (OR; left panel gold) and tract (OT; left panel, magenta) from probabilistic tractography (Ogawa et al., 2014). Estimates of fractional anisotropy (FA) projected on top of the anatomy of the OR and OT (right panel). **B** Measurement of FA averaged across the length of the left optic radiation in A. **C**. Matrix of connections between several cortical brain areas. The connection value in each cell of the matrix was derived by normalizing the number of fascicles touching two regions (Sporns, 2013).

2 Tracts and connections across human visual maps

The spatial arrangement of retinal inputs is maintained in visual cortex; signals from nearby locations in the retina project to nearby locations in cortex (Henschen, 1893; Holmes and Lister,

1916; Inouye, 1909; Wandell et al., 2007; Wandell and Winawer, 2011). Vision scientists routinely use functional magnetic resonance imaging (fMRI) to identify these visual field maps (Engel et al., 1994; DeYoe et al., 1994; Sereno et al., 1995; Dumoulin and Wandell, 2008), and more than 20 maps have been identified to date (Smith et al., 1998; Press et al., 2001; Brewer et al., 2005; Larsson and Heeger, 2006; Amano et al., 2009; Arcaro et al., 2009; Silver and Kastner, 2009; Wandell and Winawer, 2011). Recent advances in dMRI and tractography are opening new avenues to study connections between visual field maps through the white matter in living brains. This section introduces what we can learn from relating visual field maps with the endpoints of the white matter pathways.

Segregation, clustering and hierarchy in visual field maps

The functional organization of the visual field maps in humans and animal models has been identified by convergent knowledge from fMRI, neuropsychological and cytoarchitectonic studies (Wandell et al., 2007; Wandell and Winawer, 2011; Vanduffel et al., 2014; Kolster et al., 2014). We propose three organizational principles for the architecture of the visual field maps to summarize findings in the literature: segregation, clustering and hierarchy. The first principle proposes that visual maps have some degree of functional specialization. This is a soft principle because many areas deal with multiple aspects of the visual stimulus, but some areas respond with more stimulus specificity than others (e.g. motion selectivity in macaque MT and human MT+; (Dubner and Zeki, 1971; Movshon et al., 1985; Watson et al., 1993; Tootell et al., 1995; Huk and Heeger, 2002). There is a classic proposal that functional segregation might extend beyond single visual maps. It has been proposed that visual field maps can be grouped into a dorsal and a ventral stream (Ungerleider and Mishkin, 1982; Ungerleider and Haxby, 1994; Milner and Goodale, 1995). According to this model, the dorsal stream engages in spatial processing and action guidance, whereas the ventral stream engages in analyzing colors and forms. The second principle organizes visual field maps into clusters which share common eccentricity maps (Wandell et al., 2007; Kolster et al., 2014, 2009) and are distinguished by their angular representations. The third principle identifies a hierarchy of visual field maps (Felleman and Van Essen, 1991) based on the input and output layer projections. The first and third principles were defined mostly based on tracer injections, neurophysiological measurements and cytoarchitecture in the macaque brain. The second principle was discovered using functional MRI which has a large field of view and thus can visualize large-scale topological organization of visual field maps.

Functional segregation, clustering and hierarchy are likely to be established by both cortical neuronal sensitivity properties and the connectivity of neurons communicating across different maps. To date, the full anatomical structure of connections of the human visual cortex has not been characterized. This structure is likely to differ between macaque and human brain because the visual field map organization and cortical mantle anatomy differ between the two species in several ways (Vanduffel et al., 2014; Wandell and Winawer, 2011).

Understanding the network of communication pathways in the human brain is fundamental to understanding visual function in health and disease. Building a model of the communication architecture will also help with both prognosis and intervention, this is because vision is a sense that integrates information across many visual features (Huk and Heeger, 2002). For example, skilled reading requires the integration of information across visual space, spatial attention, eye movements, as well as word recognition (Vidyasagar and Pammer, 2010). In fact, there is converging evidence showing the possibility of communication between dorsal and ventral streams (Fang and He, 2005; Grill-Spector et al., 1998, 2000; James et al., 2002; Konen and Kastner, 2008), although the anatomy of white matter pathway communicating these maps clusters was not well understood

until very recent reports (see below).

Relating structure to function: Combining fMRI and diffusion MRI to identify the tracts communicating between maps

There are several examples combining fMRI and dMRI to clarify the relationship between the white matter tracts and visual field maps. Dougherty and colleagues analyzed the relationship between the visual field maps and corpus callosum fascicles (Dougherty et al., 2005). This analysis was extended to measure the properties of this pathway in relation to reading (Dougherty et al., 2007) and blindness (Saenz and Fine, 2010; Bock et al., 2013). Kim and colleagues explored white matter pathways between early visual cortex and category selective regions by combining fMRI, dMRI and fiber tractography (Kim et al., 2006). Greenberg and colleagues identified the visual field maps in intraparietal sulcus using fMRI (Silver and Kastner, 2009) and analyzed the tracts communicating IPS maps and early visual field maps (Greenberg et al., 2012). There are studies attempting to identify the pathway between subcortical nuclei (LGN or Pulvinar) and cortical maps (Ajina et al., 2015; Alvarez et al., 2015; Arcaro et al., 2015).

Validating novel tracts

Whereas these approaches provide novel insight on the relationship between white matter pathway and functionally-defined cortical maps, a statistical evaluation can clarify how much the white matter connection between maps are supported by dMRI data increasing the confidence in visual white matter organization identified by dMRI. Pestilli and colleagues developed a method in which the evidence in support of a fascicle of interest is quantified by comparing model accuracy with and without the fascicle (Pestilli et al., 2014). This analysis is used to evaluate the statistical evidence for relatively unstudied pathways, including pathways between visual areas (Gomez et al., 2015; Leong et al., 2016; Takemura et al., 2015).

We used this approach to study the Vertical Occipital Fasciculus (VOF). The VOF, which connects dorsal and ventral visual field maps, was known to 19th century anatomists from post-mortem studies (Wernicke, 1881; Sachs, 1892; Déjerine, 1895), but it was widely ignored in the vision literature until recent studies primarily using dMRI (Yeatman et al., 2013; Martino and Garcia-Porrero, 2013; Yeatman et al., 2014b; Takemura et al., 2015; Duan et al., 2015; Weiner et al., 2016). By combining fMRI and dMRI it is possible to visualize the VOF endpoints near the visual field maps (Takemura et al., 2015).

Figure 8C describes the endpoints of the VOF overlaid on the cortical surface together with visual field map boundary identified in Figure 8A. We plotted the position of grey matter nearby the tract endpoints in color maps on cortical surface. The dorsal endpoints of the VOF are near V3A, V3B and neighboring maps(Figure 8C; (Takemura et al., 2015)). The ventral endpoints of the VOF are near hV4 and VO-1. This is important because it sheds light on the nature of communication through the VOF: hV4 and VO-1 are the first full hemifield maps in the ventral stream (Wade et al., 2002; Brewer et al., 2005; Arcaro et al., 2009; Winawer and Witthoft, 2015; Winawer et al., 2010), while V3A and V3B are the first visual field maps to contain a full hemifield representation in the dorsal stream. V3A and V3B also have an independent foveal cluster (Smith et al., 1998; Press et al., 2001) and respond selectively to motion and to disparity (Tootell et al., 1997; Backus et al., 2001; Tsao et al., 2003; Nishida et al., 2003; Ashida et al., 2007; Cottereau et al., 2011; Fischer et al., 2012; Goncalves et al., 2015).

We note that there are some limitations to associating “tract endpoints” in tractography and cortical projections in gray matter. In practice, tractography is usually terminated at the boundary

between gray and white matter, because standard dMRI measurements fall under the resolution required to accurately delineate the complex tissue organization within gray matter. Therefore, there is uncertainty in relating tract endpoints to the cortical surface. This uncertainty is compounded by the dispersion of axons in gray matter, and by U-fiber system in superficial white matter which impedes accurate estimation of tract endpoints (Reveley et al., 2015). Thus, the analysis will give us the information on the spatial proximity between tract endpoint and cortical maps, but does not provide us a definitive estimate on the cortical projection of the tract. We may expect the improvement of the quality of this analysis by utilizing the modelling of complex fiber organization from diffusion MRI data, improving data resolution (Sotiropoulos et al., 2013) or improved tractography methods (Reisert et al., 2011; Takemura et al., 2016; Wandell, 2016).

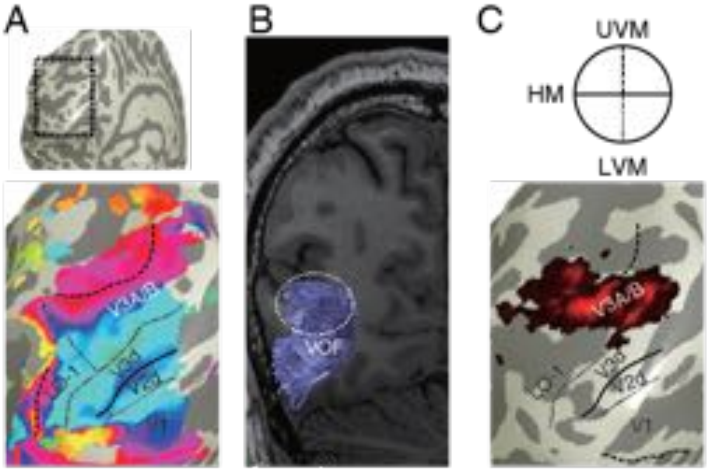

Figure 8: Relation between cortical visual field maps and tract endpoints. **A** Visual field maps identified by fMRI. The surface of dorsal visual cortex was extracted (dotted box in top panel) and enlarged (bottom panel). Colors on the bottom panels describes polar angle representation in population receptive field maps (Dumoulin and Wandell, 2008) red: upper vertical meridian, blue: horizontal, green: lower vertical meridian). The boundaries between visual field maps are defined as polar angle reversals in population receptive field maps. **B** The VOF identified in an identical subject using dMRI and fiber tractography. Reproduced from (Takemura et al., 2015) with permission. **C** Overlay between visual field maps and VOF projections. Color maps indicate voxels near the VOF endpoints in this hemisphere, and the color scale indicates the density of fascicle endpoints. The borders of visual field maps (solid and dotted lines; upper panel depicts the representation of horizontal and vertical meridians) were adopted from fMRI-based mapping (**A**).

3 Relationship between the visual white-matter and visual impairment

One of the motivations for studying the effects of blindness on white matter, is that our extensive understanding of the anatomical and functional structure of the visual system, both in visually normal and in visually deprived animals, provides a good model system in which to evaluate current methods for measuring white matter structure in vivo. Indeed since the classic studies of Hubel and Wiesel in the 1960s (Wiesel and Hubel, 1963, 1965b,a; Wiesel et al., 1963), visual deprivation has been an important model for examining the effects of early experience on brain development and function. In this section, we focus on the effects of visual loss, due to peripheral blindness (such as retinal disease), on white matter pathways. In addition, we discuss how in vivo measurements of white matter structure can provide insight into pathways that mediate blindsight after striate lesions. Blindsight provides a particularly elegant example of determining which of multiple candidate pathways are likely to mediate residual behavioral performance based on in vivo measurements of white matter structure.

White matter changes due to peripheral blindness

Visual deprivation resulting from loss of input from the eye provides an excellent model for understanding the links between structure and function, as the brain itself remains largely intact. A wide variety of studies in both animals and humans have demonstrated large scale functional (Lewis and Fine, 2011), neuroanatomical (Bock and Fine, 2014; Movshon and Van Sluyters, 1981), neurochemical (Coullon et al., 2015; Weaver et al., 2013) and even vascular (De Volder et al., 1997; Uhl et al., 1993) changes within occipital cortex as a result of early blindness. Given this extensive animal and human literature, peripheral blindness provides a particularly good model system to examine the reliability and sensitivity of current noninvasive methods for assessing the effects of experience on white matter pathways. Here, we review the white matter changes associated with visual deprivation, paying particular attention to the links between white matter microstructure and alterations of functional responses due to visual loss.

The optic tract and optic radiations

Early or congenital blindness results in severe degradation of the optic tract (between the eye and the lateral geniculate nucleus) and the optic radiations (between the lateral geniculate nucleus and V1). Not only are these pathways noticeably reduced in volume, but there is also decreased longitudinal and increased radial diffusivity within these tracts (Noppeney et al., 2005; Ptito et al., 2008; Reislev et al., 2015; Shu et al., 2009) suggesting degradation of white matter microstructure within the remaining tract. These effects seem to be particularly pronounced in anophthalmic individuals, suggesting that retinal signals play a role in the development of these tracts (Bridge et al., 2009).

Reductions in fractional anisotropy (FA) within the optic tract and optic radiations are also found in individuals who become blind in adolescence or adulthood (Dietrich et al., 2015; Shimony et al., 2006; Wang et al., 2013). There is some suggestion that the microstructure of these tracts may be more heavily degraded in individuals with acquired blindness than in congenitally blind individuals, though in some part these results may be due to the etiologies of later blindness - for example glaucoma is capable of causing physical damage to the optic tract.

Callosal connectivity

Despite numerous studies, the effects of early visual deprivation on the posterior callosal fibers within the splenium (connecting the occipital lobes) are not yet fully understood. Several studies (Leporé et al., 2010; Ptito et al., 2008; Tomaiuolo et al., 2014) have reported that the posterior part of the corpus callosum is reduced in volume. However, Bock et al. (2013) failed to find any indication of reduced volume in the portion of the splenium containing fibers connecting V1/V2 in either early blind or anophthalmic individuals (Bock et al., 2013). In the Bock et al. study, the only evidence of callosal atrophy due to visual loss was a slight reduction in FA within the splenium in anophthalmic individuals. Given the magnitude of the effect found by Tomaiuolo et al., the Bock study may have been underpowered, though there was no indication of a non-significant difference between groups. An alternative possibility is that the significant methodological differences across the studies may explain the discrepancy in results. Most of the studies listed above registered individual data to a template, with some studies then anatomically segmenting the callosum into sub-regions of various sizes. In contrast, Bock et al. defined the splenium in a midline sagittal slice using fibers tracked from a surface based ROI, in which V1/V2 was identified based on cortical folding for each subject – resulting in a much more restrictive definition of the splenium. Indeed, the splenial region of interest in the Bock et al. (2013) study was roughly a third of the area defined by Tomaiuolo et al. (Tomaiuolo et al., 2014). Thus, one possible explanation for these differing findings is that the callosal fibers that connect V1/V2 are less affected by visual deprivation than those representing higher-level cortical areas.

As well as examining the volume of the splenium, Bock et al. (2013) also showed that the topographic organization of occipital fibers within the splenium is maintained in early blindness. Even within anophthalmic individuals, it was possible to observe a ventralâĂŞdorsal mapping within the splenium with fibers from ventral V1-V3 (representing the upper visual field) projecting to the inferior-anterior corner of the splenium and fibers from dorsal V1-V3 (representing the lower visual field) projecting to the superior-posterior end. Similarly, it was possible to observe an eccentricity gradient of projections from foveal-to peripheral V1 subregions running in the anterior-superior to posterior-inferior direction, orthogonal to the dorsal-ventral mapping(Bock et al., 2013).

Cortico-cortical connections

Over the last two decades a considerable number of studies have observed functional cross-modal plasticity (novel or augmented responses to auditory or tactile stimuli within occipital cortex) as a result of congenital blindness. Specifically, occipital regions have been shown to demonstrate functional responses to a variety of auditory (Röder et al., 1999; Lessard et al., 1998; Voss et al., 2004; Gougoux et al., 2004; Jiang et al., 2014), language (Sadato et al., 1996; Cohen et al., 1997; Röder et al., 2002; Burton et al., 2003; Bedny et al., 2011; Watkins et al., 2012) and tactile (Alary et al., 2009; Goldreich and Kanics, 2003; Van Boven et al., 2000) stimuli. One of the more attractive explanations for these cross-modal responses, given the animal literature (Innocenti and Price, 2005; Restrepo et al., 2003; Webster et al., 1991), is that they might be mediated by altered white matter connectivity – for example a reduction in experience-dependent pruning. As a result, when methods for measuring white matter tracts in vivo became available there was immediate interest in looking for evidence of novel and/or enhanced connections within early blind individuals. However, despite the massive changes in functional responses within occipital cortex that are observed as a result of blindness, cortico-cortico white matter changes as a result of early blindness are not particularly dramatic, with little or no evidence for enhanced connectivity as predicted by the 'reduced pruning' hypothesis.

Indeed, reduced fractional anisotropy is consistently found within white matter connecting the occipital and temporal lobes (Bridge et al., 2009; Ptito et al., 2008; Reislev et al., 2015; Shu et al., 2009). This finding is somewhat puzzling given that several studies have shown that language stimuli activate both the lateral occipital cortex and fusiform regions in congenitally blind individuals (Bedny et al., 2011; Watkins et al., 2012). Similarly, no increase in FA has been detected in the pathways between occipital and superior frontal cortex, a network that has shown to be activated by language in congenitally blind populations (Bedny et al., 2011; Watkins et al., 2012) (Bedny et al., 2011; Watkins et al., 2012). Indeed two studies have found evidence of deterioration (e.g. reduced FA) within the inferior fronto-occipital fasciculus (Reislev et al., 2015; Shu et al., 2009).

It is not clear what causes the lack of consistency in the studies described above. One likely factor is between-subject variability. Estimates of individual differences in tracts suggest that between-group differences require surprisingly large subject numbers even for relatively large and consistently located tracts. For example, within the inferior and superior longitudinal fasciculus, to detect a 5% difference in fractional anisotropy at 0.9 power would require 12-19 subjects/group in a between-subject design (Veenith et al., 2013) . Because of the difficulty of recruiting blind subjects with relatively homogenous visual histories, many of the studies cited above used moderate numbers of subjects.

One of the more puzzling findings described above is the consistent finding of reduced white connectivity between occipital and temporal lobes and between occipital and superior frontal lobes, given that occipital cortex shows enhanced responses to language as a result of blindness. One possibility is that measured connectivity provides a misleading picture of actual connectivity between these regions. One potential confound is the effect of crossing fibers. If blindness leads to a loss of pruning that extends beyond these major tracts then the resulting increase in the prevalence of crossing fibers within other networks might reduce measurable FA within occipito-temporal and occipito-frontal tracts.

Alternatively, it is possible that the enhanced language responses found in occipital cortex genuinely co-exist with reduced connectivity with temporal cortex. For example, we have recently suggested that an alternative perspective in understanding cortical plasticity as a result of early blindness is to consider that occipital cortex may compete rather than collaborate with non-deprived regions of cortex for functional role (Bock and Fine, 2014). According to such a model, lateral occipital cortex may compete with temporal areas, with language tasks assigned to the two regions in such a way as to maximize the decoupling between the areas. In the context of such a framework, reductions in anatomical connectivity between the two areas are less surprising.

Early vs. late blindness

Reductions in fractional anisotropy (FA) within the optic tract and optic radiations are also found in individuals who become blind in adolescence or adulthood (Dietrich et al., 2015; Shimony et al., 2006; Wang et al., 2013), suggesting that visual input is necessary for maintenance as well as development of these tracts. Indeed, there is some suggestion that the microstructure of these tracts may be more heavily degraded in individuals with acquired blindness than in congenitally blind individuals, though in some part these results may be due to the etiologies of later blindness - for example glaucoma is capable of causing physical damage to the optic tract.

The effects of early vs. late blindness on cortico-cortico white matter connections remains unclear. One study has found that reductions in FA may be more widespread in late acquired blindness compared to congenital blindness, with late blind individuals showing reduced FA in the corpus callosum, anterior thalamic radiations, and frontal and parietal white matter regions

(Wang et al., 2013). Such a result is quite surprising, though it is possible that the cross-modal plasticity that occurs in early blind individuals might prevent deterioration within these tracts, and this 'protective' effect does not occur in late blind individuals. However this difference between late and early blind subject groups was not replicated by Reislev et al. (Reislev et al., 2015) who noted similar losses in FA for early and late blind subjects within both the inferior longitudinal fasciculus and the inferior fronto-occipital fasciculus using a tract-based approach. (This group did find that significant increases in radial diffusivity within late blind subjects relative to sighted control subjects, but did not directly compare radial diffusivity between late and early blind subject groups.)

White matter changes due to cortical blindness

Damage to the primary visual cortex (V1) causes the loss of vision in the contralateral visual field (homonymous hemianopia), which in turn leads to degeneration of the geniculo-striate tract. Despite these lesions and a lack of conscious vision, many people can still correctly detect the presence/absence of a stimulus (Poppel et al., 1973), as well as discriminate between variations in stimulus color and motion, (Ffytche et al., 1996; Morland et al., 1999) despite a lack of conscious awareness of the stimulus – a condition known as 'blindsight' (Poppel et al., 1973; Weiskrantz et al., 1974). Given the absence of the major geniculo-striate projection, any residual visual information is likely to be conveyed by an intact projection from subcortical visual regions to undamaged visual cortex.

While several individual case studies have examined the white matter pathways underlying residual vision (Bridge et al., 2010, 2008; Leh et al., 2006; Tamietto et al., 2012), a critical test of the functional relevance of white matter microstructure was recently carried out by comparing individuals with V1 lesions who did and did not demonstrate residual 'blindsight' vision. Ajina et al. (2015) examined white matter microstructure within three potential pathways that might subserve residual vision in hemianopia patients. They showed that two potential pathways (superior colliculus to hMT+ and the interhemispheric connections between hMT+) did not differ in microstructure between those with and without blindsight. In contrast, the pathway between LGN and hMT+ in the damaged side differed significantly across individuals with and without blindsight. Patients with blindsight had comparable FA and MD in damaged and intact hemispheres. Patients without blindsight showed a loss of structural integrity within this tract in the damaged hemisphere (Ajina et al., 2015). These results provide an elegant example of how white matter microstructure measurements can be correlated with visual function in order to infer structure-function relationships.

Summary

Within the subcortical pathways, our review of the literature suggests that in vivo measurements of white matter microstructure can provide sensitive and reliable measurements of the effects of experience on white matter. Studies consistently find the expected deterioration within both the optic tract and the optic radiations in the case of peripheral blindness. Similarly, analysis of subcortical pathways in blindsight have shown consistent results across several cases, and are interpretable based on the functional and pre-existing neuroanatomical literature.

In contrast, it has proved surprisingly difficult to obtain consistent results for measurements of cortico-cortico connectivity across different studies. These discrepancies in the literature are somewhat surprising given the gross differences in visual experience that occurs in early and even late blind individuals. One possible explanation is that, as described above, most studies (though with a few exceptions, e.g. Wang et al. (2013)) have tended to have relatively low statistical

power. Larger sample sizes (perhaps through a multi-center study) might better reveal more subtle anatomical differences in connectivity as a result of early blindness. A second factor may be methodological differences across studies – early blind subjects are anatomically distinct within occipital cortex – for example occipital cortex shows less folding in animal models (Dehay et al., 1996), which may affect estimates of white matter tracts that are based on methods involving normalization to a canonical template. Comparing results based on tracts identified based on normalization to anatomical templates to those obtained using tracts identified within individual anatomies may provide some insight into how these very different approaches compare in terms of sensitivity and reliability.

It has also proved surprisingly difficult to interpret alterations in white matter cortico-cortico connectivity in the context of the functional literature – occipito-temporal and occipito-frontal white matter connections have consistently been shown to be weaker in early blind subjects, despite the apparent recruitment of occipital cortex for language. This discrepancy between estimates of white matter connectivity and functional role within cortico-cortical tracts makes it clear that drawing direct conclusions from white matter microstructure to functional role is still fraught with difficulty. This is not a reason to abandon the enterprise, but rather provides a critical challenge. To return to the argument with which we began this chapter – the effects of visual deprivation provide an excellent model system for testing how well we understand the measurement and interpretation of in vivo measurements of white matter infrastructure.

4 Properties of white matter circuits involved in face perception

In the visual system, neural signals are transmitted through some of the most prominent long-range fiber tracts in the brain: the optic radiations splay out from the thalamus to carry visual signals to primary visual cortex; the forceps major, u-shaped fibers that traverse the splenium of the corpus callosum, innervate the occipital lobes allowing them to integrate neural signals; the inferior longitudinal fasciculus (ILF) is the primary occipito-temporal associative tract (Crosby, 1962; Gloor, 1997) that propagates signals through ventral visual cortex between primary visual cortex and the anterior temporal lobe (see Figure 9a); and, finally, the inferior fronto-occipital fasciculus (IFOF) begins in the occipital cortex, continues medially through the temporal cortex dorsal to the uncinate fasciculus, and terminates in the inferior frontal and dorsolateral frontal cortex (see Figure 9a; Catani et al. (2002). Increasingly, diffusion neuroimaging studies are providing evidence indicating the importance of these white matter tracts for visual behavior. Here, we present evidence from converging streams of our research demonstrating that the structural properties of the ILF and IFOF are critically important for intact face perception.

Face perception is a complex suite of visual behaviors that is subserved by a distributed network of neural regions, many of which are structurally connected by the ILF and IFOF. For example, the “core” or posterior regions include the occipital face area (OFA), the fusiform face area (FFA), and the posterior superior temporal sulcus (pSTS) and the “extended” areas include the anterior temporal pole (ATP), amygdala, and ventro-medial prefrontal cortex (vmPFC) (Gobbini and Haxby, 2007). Recently, functional neuroimaging studies have provided supporting, albeit indirect, evidence of rapid interactions between these posterior core regions and the extended anterior regions (e.g., anterior temporal lobe and amygdala) that implicate the involvement of long-range association fiber tracts that connect these regions, including the ILF and the IFOF (Bar et al., 2006; Gschwind et al., 2012; Rudrauf et al., 2008; Song et al., 2015).

Finally, damage to either of these pathways disrupts face processing (Catani et al., 2003; Catani and Thiebaut de Schotten, 2008; Fox et al., 2008; Philippi et al., 2009; Thomas et al.,

2009), suggesting that these white matter tracts serve as a critical component of the neural system necessary for face processing. In what follows, we provide evidence showing that age-related changes in the structural properties of these tracts in early development is associated with emergent properties of the functional neural network supporting face processing. We also review evidence that age-related decreases in the structural properties of these tracts in aging adults exist and are associated with decrements in face processing behavior. Finally, we review data showing that relative deficits in the structural properties of these long-range fiber tracts potentially explain the causal nature of face blindness in individuals with congenital prosopagnosia. Together these findings converge to indicate that the structural properties of white matter tracts, and the ILF and IFOF in particular, are necessary for skilled face perception.

Across all of these studies, we use a common methodological approach. We acquire diffusion images, analyze them using a tensor model, and perform deterministic tractography using the Fiber Assignment of Continuous Tracking (FACT) algorithm and brute-force fiber reconstruction approach (Mori et al., 1999; Xue et al., 1999) with fairly standard parameters. To extract the tracts of interest, we use a multiple region of interest (ROI) approach that is very similar to Wakana et al (Wakana et al., 2007). From each tract, we extract the volume (the number of voxels through which the fibers pass multiplied by the volume of the voxel) as well as the mean fractional anisotropy (FA), mean diffusivity (MD), axial diffusivity (AD), and radial diffusivity (RD) values across these voxels.

Age-related changes in the ILF and IFOF with functional neural change

The central question guiding this work was whether developmental differences in the structural properties of the ILF and IFOF, defined independently using anatomical ROIs, are related to developmental differences in the characteristics of the functional face-processing regions connected by these tracts (Scherf et al., 2014). Across participants whose ages covered a substantial range (ages 6-23 years), we evaluated differences in (1) the macro- and microstructural properties of the fasciculi, and in (2) the functional profile (size, location, and magnitude of selectivity) of the face- and place-selective regions that are distributed along the trajectory of the pathways of interest using functional magnetic resonance imaging (fMRI). First, we found that all tracts, with the exception of the left IFOF, exhibited age-related improvements in their microstructural properties, evincing a significant decrease in mean and radial, but not axial, diffusivity from childhood to early adulthood (see Figure 9b). This result is consistent with the idea that the increasingly restricted diffusion perpendicular to the axons in these tracts reflects continued myelination from childhood through early adulthood. The left IFOF exhibited stable levels of microstructural properties across the age range, indicating that it may be a very early developing fiber tract. At the macro-structural level, only the ILF exhibited an age-related change in volume, which was evident in both hemispheres. The combined increases in micro-structural properties and the volume of the right ILF suggest that it is becoming increasingly myelinated and/or more densely packed with axons with age (Beaulieu, 2002; Lebel and Beaulieu, 2011; Song et al., 2005).

Having identified the structural changes that potentially contribute to circuit organization, we explored, concomitant differences in the functional profile of face-related cortical regions, and then examined the joint structure-function correspondences. Across the full age range, individuals with larger right FFA volumes also exhibited larger right ILF volumes (see Figure 9c). Neither the right OFA nor the right PPA exhibited this structure-function relation with the right ILF. This structure-function relation between the right FFA and right ILF was also present in just the children and adolescents (aged 6-15 years). However, once age was accounted for in the same model as size of the right FFA in the children and adolescents, the age effects on the volume of the ILF swamped all the significant variation, even though the size of the right FFA increased significantly

683 across this age range. One interpretation of these findings is that the neural activity generated by
684 larger functional regions may require and/or influence the development of larger fiber tracts (via
685 increasing myelination of existing axons and/or more densely packed axons) to support the trans-
686 mission of neural signals emanating from such regions. It may also be that increasing the integrity
687 of the structural architecture of fiber tracts increases the propagation of neural signal throughout
688 the circuit, thereby enhancing the functional characteristics of the nodes within the circuit (and
689 vice versa). In other words, structural refinements of white matter tracts may precede, and even
690 be necessary for, functional specialization of the circuit to emerge. In sum, this work uncovers the
691 key contributions of the ILF and IFOF and their relationship to functional selectivity in the develop-
692 ing circuitry that mediates face perception. Aging related decrease in structural properties of IFOF
693 with face perception deficits While the findings above focus on understanding how the structural
694 properties of the ILF and IFOF are critical for building the complex face processing network during
695 early development, it was also important to understand whether disruptions in these white matter
696 tracts might be associated with, or even responsible for, age-related declines in face processing
697 that are well reported (e.g., Salthouse (2004)) and are not solely a function of memory or learning
698 changes (Boutet and Faubert, 2006). We scanned 28 individuals aged 18-86 years using a diffu-
699 sion tensor imaging protocol (Thomas et al., 2008). We also tested them in face and car perceptual
700 discrimination tasks. We observed that the right IFOF was the only tract that decreased in volume
701 (as measured by percent of fibers and voxels through which the fibers pass) as a function of age.
702 In contrast, the bilateral IFOF and the left, but not right, ILF exhibited age-related decreases in
703 FA (see Figure 9d). To summarize, it is the IFOF in the right hemisphere that shows particular
704 age-related vulnerability, although there is a tendency for the tracts in the left hemisphere to show
705 some reduction in microstructural properties, as revealed in FA values, as well.

706 On the discrimination tasks, participants performed more poorly on the difficult trials, especially
707 in the face compared to the car condition. Of relevance though is that the older individuals, the 60-
708 and 80-year-olds, made significantly more errors on faces than they did on cars, and performance
709 was almost at chance in the difficult condition. Given that there were age-related declines in the
710 micro- and macro-structural properties of the IFOF as well as in face perception behavior, our
711 final question was whether there was an association between these tract and behavioral deficits.
712 To address this question, we examined correlations between behavioral performance and the
713 normalized percentage of fibers, normalized percentage of voxels and average FA values in the
714 ILF and IFOF in each hemisphere. We observed two main findings: a. during the easy face trials,
715 participants with greater percentage of fibers in the right IFOF, exhibited better performance in
716 these easy discriminations and b. during the difficult face trials, participants with higher FA values
717 and larger volume right IFOF exhibited better performance on the difficult discriminations. Taken
718 together, these findings indicate a clear association between the ability to discriminate between
719 faces and the macro- and micro-structural properties of the IFOF in the right hemisphere.

720 Disruptions in ILF and IFOF may explain face blindness

721 Finally, given the findings of an association between face processing behavior and the structural
722 properties of the IFOF in typically developing adults, we investigated whether congenital prosopag-
723 nosia, a condition that is characterized by an impairment in the ability to recognize faces despite
724 normal sensory vision and intelligence, might arise from a disruption to either and/or both the ILF
725 and IFOF (Thomas et al., 2009). This hypothesis emerged following empirical findings that the
726 core functional neural regions, including the FFA, appeared to produce normal neural signals in
727 many congenital prosopagnosic individuals (Avidan et al., 2014, 2005; Thomas et al., 2009). To
728 test this hypothesis, we scanned 6 adults with congenital prosopagnosia, all of whom evinced

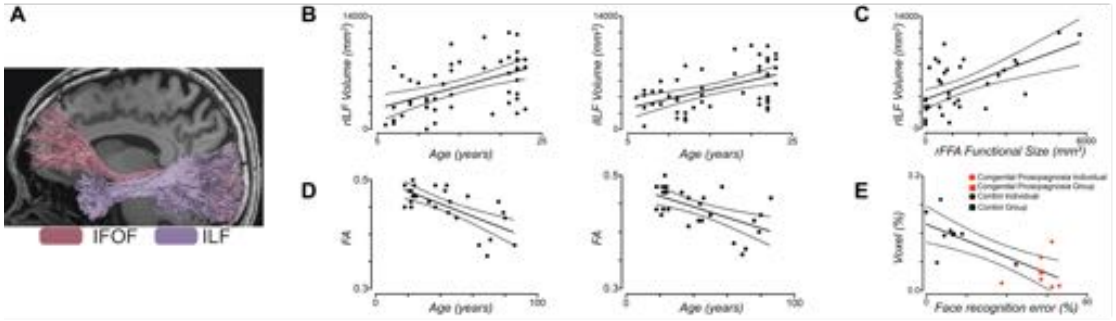

Figure 9: The Role of the ILF and IFOF in face perception. **A** Representative example of fibers extracted from the inferior longitudinal fasciculus (ILF), which is the primary occipito-temporal associative tract (Crosby, 1962; Gloor, 1997) that propagates signals through ventral visual cortex between primary visual cortex and the anterior temporal lobe; and, from the finally, the inferior fronto-occipital fasciculus (IFOF), which begins in the occipital cortex, continues medially through the temporal cortex dorsal to the uncinate fasciculus, and terminates in the inferior frontal and dorsolateral frontal cortex (Catani et al., 2002). **B** In typically developing individuals, there is a systematic age-related increase in the macro-structural properties of both the right and left ILF, which is measured here by the volume of the tract in cubic millimeters, across the first two decades of life. **C** We observed a joint structure-function correspondence between the size of the individually defined functional right fusiform face area and the volume of the right ILF, which held even when age was accounted for (Scherf et al., 2014). **D** In typically developing adults, there is a systematic age-related decline in the micro-structural properties of both the right and left IFOF, as measured by the mean FA, indicating that it is disproportionately vulnerable compared to the ILF during the aging process. **E** Individuals who have a lifetime history of face blindness, an inability to recognize faces in spite of normal intelligence and sensory vision, have systematically smaller volume visual fiber tracts, particularly in the right ILF, as depicted here, compared to age-matched control participants. Together, these findings provide converging evidence that these two major tracts, the IFOF and the ILF, carry signals important for face perception.

normal BOLD activation in the core face regions (Avidan et al., 2005), and 17 age- and gender-matched control adults. We also measured participants' face recognition skills. Relative to the controls, the congenital prosopagnosia (CP) group showed a marked reduction in both the macro- and micro-structural properties of the ILF and IFOF bilaterally. We then carried out a stepwise regression analysis with the connectivity and behavioral measures. Across participants, individuals with the worse face recognition behavior had the lowest FA and smallest volume right ILF (see Figure 10e). Similarly, poor face recognition behavior was also related to smaller volume of the right IFOF, as well. In summary, our study reveals that the characteristic behavioral profile of congenital prosopagnosia may be ascribed to a disruption in structural connectivity in some portion of the ILF and, perhaps to a lesser extent, the IFOF (for related findings, see Gomez et al. (2015); Song et al. (2015)).

Summary

We have presented converging evidence that face recognition is contingent upon efficient communication across disparate nodes of a widely distributed network, which are connected by long range fiber tracts. Specifically, we have shown that two major tracts, the IFOF and the ILF, carry signals important for face perception. Studies in children and older individuals, as well as investigations with individuals who are face blind all attest to the required integrity of the tracts for normal face recognition behavior. Early in development the ILF undergoes a particularly long trajectory in which both the micro- and macro-structural properties change in ways indicative of increasing myelination. Of relevance for the integrity of face perception behavior, there is a highly selective and tight correspondence between age-related growth in one of the pre-eminent functional nodes of the face-processing neural network, the right FFA, and these age-related improvements in the structural properties of the ILF. These findings reflect the dynamic and intimate nature of the relation between brain structure and function, particularly with respect to role of white matter tracts, in setting up neural networks that support complex behaviors like face perception. Our work with congenital prosopagnosic participants suggests that face-processing behavior will not develop normally when this developmental process is disrupted. Future work will need to identify when, developmentally, white matter disruptions are present and interfere with face perception. Finally, our work in aging adults indicates that the IFOF, is particularly vulnerable with age, which can lead to difficulties with face recognition behavior. However, Grossi and colleagues (Grossi et al., 2014) reported that an adult with progressive prosopagnosia, a gradual and selective inability to recognize and identify faces of familiar people, had markedly reduced volume ILF in the right, but not left hemisphere, whereas the bilateral IFOF tracts were preserved. This suggests that there may be some conditions in adulthood in which the ILF is also vulnerable. Together, these findings converge on the claim that the structural properties of white matter circuits are, indeed, necessary for face perception.

5 Conclusions, remarks and future directions

The goal of the present article is to survey the range of findings about the specific importance of studying the white matter of the visual system. We focused on findings in human brains, that used the only currently available method to study the white matter in vivo in humans: diffusion MRI (dMRI). In the time since its invention in the 1990's, dMRI methods have evolved, and evidence about the importance of the white matter has accumulated (Fields, 2008b). These findings are modern, but they support a point of view about the nervous system that has existed for a long time. Connectionism, the theory that brain function arises from its connectivity structure goes back to classical work of the 19th century neurologists (Deacon, 1989). Over the years, interest in disconnection syndromes waxed and waned, as more holistic views of the brain (Lashley, 1963) and more localizationist views of the brain prevailed. As a consequence, systems neuroscience has traditionally focused on understanding the response properties of individual neurons and cortical regions (Fields, 2013, 2004). Only a few studies were devoted to understanding the relation of the white matter to cognitive function. Similar to electrical cables, it was believed that the connections in the brain were either intact and functioning, or disconnected. However, the pendulum started swinging back dramatically towards connectionism already in the 1960's (Geschwind, 1965), and over the years, there has been increasing appreciation for the importance of brain networks in cognitive function, culminating in our current era of connectomics (Sporns et al., 2005). In addition to an increasing understanding of the importance of connectivity, views that emphasize the role

of tissue properties not related to neuronal firing in neural computation have more recently also evolved and come to the fore (Bullock et al., 2005; Fields, 2008b). For example, the role of glial cells in modulating synaptic transmission and neurotransmitter metabolism, as well as the role of the white matter in metabolism and neural hemodynamic coupling (Robel and Sontheimer, 2016). Today, we know much more about the white matter than ever before and we understand that the properties of the tissue affect how communication between distal brain areas is implemented. Diffusion MRI enables inferences about the properties of the white matter tissue in vivo, which in turn enables inferences about the connection between behavior and biology.

As we have seen in the examples presented above, dMRI is a useful method to study the biological basis of normal visual perception, to glean understanding about the connectivity that underlies the organization of the visual cortex, about the breakdowns in connectivity that occur in different brain disorders, and about the plasticity that arises in the system in response to visual deprivation. But while the findings reviewed above demonstrate the importance of the white matter in our understanding of the visual system and the biological basis of visual perception, they also serve as a demonstration of the unique capacity of vision science to study a diverse set of phenomena across multiple levels of description. This is largely an outcome of the detailed understanding of different parts of the visual system, and attributable to the powerful quantitative methods that have developed in the vision sciences to study the relationship between biology and perception. For these reasons the visual system has historically proven to be a good testing ground for new methodologies. Another recurring theme of the examples presented above is the importance of convergent evidence in cognitive neuroscience (Ochsner and Kosslyn, 1999). Studies of the human visual white matter exemplify this: evidence from behavior, from functional MRI, from developmental psychology, and from physiology converge to grant us a unique view about the importance of specific pathways for perception (see sections 2 and 4). For example, the response properties of different brain regions are heavily influenced by the synaptic inputs of long range connections: one might grow to better understand the response properties of dorsal visual areas, when their connection through the white matter with ventral visual areas is known (see section 2). Similarly, the role of different functional regions in the face-perception network becomes clearer when the relationship between the size of these regions, the size of the ILF and the co-development of these anatomical divisions is demonstrated (see section 4). The study of individuals with perceptual deficits or with visual deprivation demonstrates the specific importance of particular connections, and delineates the lifelong trajectory of the role of these trajectories, also revealing possibilities and limitations of brain plasticity (see sections 3). The importance of converging evidence underscores the manner in which understanding the white matter may continue to have an effect on many other parts of cognitive neuroscience, even outside of the vision sciences.

Two major difficulties recur in the descriptions of findings reviewed above: the first is an ambiguity in the interpretation of findings about connectivity. In the Introduction (1), we described the Fiber Detection Problem. The FDP creates a pervasive difficulty in the interpretation of many of the findings regarding connectivity. It limits our ability to discover new tracts with tractography, and limits the interpretation of individual differences in connectivity. Changes in tractography methods or measurement parameters may reduce the missed fascicles or the false alarms, but it does not speak to increased sensitivity in detection of white matter pathways. Indeed recent reports demonstrated that increasing the resolution of the data may be only part of the story. Unless high-quality data are also associated with an optimal choice of tracking methods important and known connections can be missed (Thomas et al., 2014). The dilemma is that the best tractography analysis method is likely to depend on the properties of the data, as well as the fascicle to be estimated. For this reason it has been proposed to use personalized approaches to tracking. For the time

being, no fixed set of rules will work in every case (Takemura et al., 2016). Nevertheless, finding major well-known tracts in individual humans is not a major problem, and can even be automated (Yendiki et al., 2011; Yeatman et al., 2012; Kammen et al., 2015).

The other difficulty relates to the interpretation of microstructural properties such as FA and MD. While these relate to biophysical properties of the tissue in the white matter, they contain inherent ambiguities. For example, FA may be higher in a specific location in one individual relative to another because of an increased density of myelin in that individual, but it may also be higher because of a decrease in the abundance of tracts crossing through this region. In the following last section, we outline a few directions that we believe will influence the future of the field, and perhaps help address some of these difficulties.

Future directions

One of the common threads across the wide array of research in human vision science using dMRI that we present and a source of frustration and confusion in reading the dMRI literature is the ambiguity in interpretation: changes in parameters of models of the tissue may be caused by different biological processes. Two promising directions that we hope will address these ambiguities in the future, or at least reduce them have to do with new developments in the measurements and modeling of MRI data in human white matter:

Biophysical models and multi b-value models

When more than one diffusion weighting b-value is collected, additional information about tissue microstructure can be derived from the data. This includes compartment models, that account for the signal as a combination of tensors (Clark and Le Bihan, 2000; Mulkern et al., 1999) or extends the Gaussian model with additional terms (so-called Diffusion Kurtosis Imaging; Jensen et al. (2005)). More recent models take into account the diffusion properties of different kinds of tissue. For example, the CHARMED model (Assaf and Basser, 2005), explicitly models intracellular water contributions to the signal and extracellular water contributions. Other models describe axon diameter distribution (Assaf et al., 2008; Alexander et al., 2010), and dispersion and density of axons and neurites (Zhang et al., 2012). However, the field is also struggling with the ambiguity of these models (Jelescu et al., 2016), and this is a very active field of research (Ferizi et al., 2016). The ultimate goal of the field in these efforts is to develop methods and models that help infer physical quantities of the tissue that are independent of the measurement device. This goal can already be achieved with other forms of MRI measurements, which we will discuss next.

Combining diffusion-weighted and quantitative MRI

Quantitative MRI refers to an ever-growing collection of measurement methods that quantify the physical properties of neural tissue, such as their density (Mezer et al., 2013) or molecular composition (Stüber et al., 2014). These methods have already been leveraged to understand the structure and properties of the visual field maps (Sereno et al., 2013; Bridge et al., 2014). Combinations of these methods with diffusion MRI can help reduce the ambiguity and provide even more specific information about tissue properties in the white matter (Stikov et al., 2011; Mezer et al., 2013; Assaf et al., 2013; Stikov et al., 2015; Mohammadi et al., 2015). For example, a recent study used this combination to study the biological basis of amblyopia (Duan et al., 2015).

Large open data-sets

The accumulation of large open datasets with thousands of participants will enable the creation of models of individual variability at ever-finer resolution (Pestilli and Franco, 2015). This will enable more confident inferences about the role of white matter in vision. The Human Connectome Project (Van Essen et al., 2013) is already well on its way to providing a data set encompassing more than a thousand participants, including not only high-quality dMRI data, but also measurements of fMRI of the visual system. Another large publicly available dataset that includes measurements of both dMRI and fMRI of visual areas is the Enhanced Nathan Klein Institute Rockland Sample (Nooner et al., 2012). Crucially, the aggregation of large data-sets can be scaled many times if a culture of data sharing pervades a larger portion of the research community (Gorgolewski and Poldrack, 2016) and as the technical tools that allow data-sharing become more wide-spread (Wandell et al., 2015).

Table 1: Publicly available data-sets for analysis of visual white matter

Data types	Number of available subjects	Acquisition parameters	Link	Relevant papers
Human Connectome Project				
Diffusion MRI, resting state functional MRI	900 (as of May 2016 – eventually 1200)	b=1000, 2000, 3000, 90 directions each, 1.25 mm^3 isotropic resolution, 3T	`http://humanconnectome.org/`	Sotiropoulos et al. (2013)
NKI Rockland Enhanced				
Diffusion MRI, fMRI (including visual area localizer)	>600 (as of July 2015)	b=1500, 137 directions, 2 mm^3 isotropic resolution, 3T	`http://fcon_1000.projects.nitrc.org/indi/enhanced/index.html`	Nooner et al. (2012)
Data supplement to "A major human white matter pathway between dorsal and ventral visual cortex"				
Diffusion MRI, ROIs of multiple visual field maps, tractography solutions	5	b=2000, 96 directions, 1.5 mm^3 isotropic resolution, 3T	`https://purl.stanford.edu/bb060nk0241`	Takemura et al. (2015)

Open source software for reproducible neuroscience

One of the challenges facing researchers that are using dMRI is the diversity of methods available to analyze the data. To facilitate the adoption of methods and the comparison between different methods, another important element in progress towards reproducible science is the transparency of the methods. The combination of article text, software and data published in the notebooks that accompany this article, demonstrates how scientific concepts and findings can be communicated in writing, and augmented by the publication of computational methods that allow reproducing some or all of the computations. This contributes to the understanding of the concepts, to scientific education, the advancement of citizen science and supports computational reproducibility (Donoho, 2010; McNutt, 2014; Stodden et al., 2014; Yaffe, 2015).

To allow this reproducibility, robust and transparent open-source implementations of the methods have become crucial. There are several open-source projects focused on dMRI, and we review only a selection here (see also Table 2 for a selection of open source software for dMRI): the FMRIB Software Library (*FSL*) implements useful preprocessing tools (Andersson and Sotiropoulos,

2016), as well as individual voxel modeling (Behrens et al., 2003) and probabilistic tractography (Behrens et al., 2007). The *MRtrix* library implements novel methods for analysis of individual data, and group analysis (Tournier et al., 2012). *Vistasoft*, *mrTools*, *AFQ* and *LiFE* (Dougherty et al., 2005; Yeatman et al., 2012; Pestilli et al., 2011; Hara et al., 2014; Pestilli et al., 2014) integrate tools for analysis of visual fMRI with tools for dMRI analysis and tractography segmentation. *Camino* provides a set of tools, with a particular focus on multi b-value analysis. *Dipy* (Garyfallidis et al., 2014) capitalizes on the vibrant scientific Python community (Perez et al., 2010) and the work of the Neuroimaging in Python community (Nipy; Millman and Brett (2007)) to provide implementations of a broad array of diffusion MRI methods, ranging from newer methods for estimation of microstructural properties (Jensen and Helpern, 2010; Portegies et al., 2015; Fick et al., 2016; Özarslan et al., 2013), methods for tract clustering and tract registration Garyfallidis et al. (2012, 2015), as well methods for statistical validation of dMRI analysis (Rokem et al., 2015; Pestilli et al., 2014).

As available data-sets grow large, another promising direction is the adoption of approaches from large-scale data analysis in neuroscience (Caiafa and Pestilli, 2015; Freeman, 2015). These methods will enable more elaborate and computationally demanding models and methods to be considered in the analysis of large, multi-participant dMRI datasets.

Table 2: A selection of open source software for dMRI analysis

License	Details	Recent release	Website	Relevant papers
MRtrix				
Open source, Mozilla Public License	Centered on implementations of methods developed by researchers at the Florey Institute and King's College (e.g., constrained spherical convolution Tournier et al. (2007))	April 15th, 2016 (v0.3.14)	`http://mrtrix.org/`	Tournier et al. (2012)
Vistasoft				
Open source GPL, but requires Matlab	Implementations of methods developed by the Stanford Vistalab	No public release cycle	`http://web.stanford.edu/group/vista/cgi-bin/wiki/index.php/Software`	Dougherty et al. (2007)
AFQ				

Continued on next page

Table 2 – continued from previous page

License	Details	Recent release	Website	Relevant papers
Open source GPL, but requires Matlab	Automated extraction of major fiber groups and quantification of statistics along their length	November 2014 (v1.2)	https://github.com/yeatmanlab/AFQ	Yeatman et al. (2012)
LiFE				
Open Source GPL, but requires Matlab	Statistical evaluation of tractography solutions	August 2013 (v0.1)	http://francopestilli.github.io/life/	Pestilli et al. (2014)
FSL (The Oxford Center for Functional MRI of the Brain Software Library)				
Open source released under a custom license, restricting commercial use	Centered on methods developed at the Oxford FMRIB,(Implementations of many preprocessing steps, as well as modeling and probabilistic tractography)	September 2015 (Version 5.0.9)	http://fsl.fmrib.ox.ac.uk/fsl/fslwiki/	Smith et al. (2004)
Diffusion Imaging in Python (Dipy)				
Open source, BSD License	Methods for voxel reconstruction, tractography, tractography segmentation, clustering and alignment, and statistical evaluation	February 2016 (v0.11)	http://dipy.org	Garyfallidis et al. (2014)
Camino				

Continued on next page

Table 2 – continued from previous page

License	Details	Recent release	Website	Relevant papers
Open source, artistic license	General analysis methods (voxel reconstruction, probabilistic tractography, etc) and specialized methods developed by the microstructure imaging at UCL, with contributions from the PICSL group at University of Pennsylvania	May 2015	http://camino.cs.ucl.ac.uk/	Cook et al. (2006)
NiftyFit				
Open source, BSD License	Diffusion and other qMRI (relaxometry) analysis methods	May 2016 (v1.3.9)	http://cmictig.cs.ucl.ac.uk/media-engagement/publications/niftyfit-multi-parametric-model-fitting-for-4	Melbourne et al. (2016)
MITK				
Open source, BSD License	Many analysis methods, including global tractography	March 2016 (v2016.03)	http://mitk.org/wiki/MITK	Wolf et al. (2005)
DTI-TK				
Open source, GPL, but requires registration	Focused on analysis methods developed at the PICSL lab (University of Pennsylvania), including white matter morphometry	October 2012	http://dti-tk.sourceforge.net/pmwiki/pmwiki.php	Zhang et al. (2010)

Acknowledgments

Ariel Rokem was funded through a grant by the Gordon & Betty Moore Foundation and the Alfred P. Sloan Foundation to the University of Washington eScience Institute Data Science Environment. Hiromasa Takemura is supported by Grant-in-Aid for JSPS Fellows. Holly Bridge is a Royal Society University Research Fellow. The work described by K. Suzanne Scherf and Marlene Behrmann

was supported by Pennsylvania Department of Health SAP grant 4100047862 (M.B., K.S.S.), NICHD/NIDCD P01/U19 (M.B., PI-Nancy Minshew), NSF grant (BCS0923763) to M.B., National Institutes of Mental Health (MH54246) to M. B., NSF Science of Learning Center grant, "Temporal Dynamics of Learning Center" (PI: Gary Cottrell, Co-I: M.B.), a post-doctoral fellowship from the National Alliance for Autism Research to K.S.S. and Beatriz Luna, and by awards from the National Alliance of Autism Research to Cibu Thomas and Katherine Humphreys and from the Cure Autism Now foundation to Katherine Humphreys. Work described by Ione Fine, Holly Bridge and Andrew Bock was funded by the National Institutes of Health (EY-014645); Holly Bridge is a Royal Society University Research Fellow. Franco Pestilli was funded by the Indiana University College of Arts and Sciences, the Indiana Clinical and Translational Institute (NIH UL1-TR001108). We thank the Jupyter team at UC Berkeley and beyond for creating the notebook format that is used in the example code provided as a computational appendix, and the Freeman Lab at HHMI Janelia Research Campus for creating the "Binder" platform to run these notebooks. We thank Kendrick Kay, Brent McPherson, Daniel Bullock, Sophia Vinci-Booher, Sandra Hanekamp, Shiloh Cooper, Brian Allen, Ian Chavez for comments on early versions of the manuscript.

References

Aganj, I., Lenglet, C., Jahanshad, N., Yacoub, E., Harel, N., Thompson, P. M., and Sapiro, G. (2011). A hough transform global probabilistic approach to multiple-subject diffusion MRI tractography. *Med. Image Anal.*, 15(4):414–425.

Ajina, S., Pestilli, F., Rokem, A., Kennard, C., and Bridge, H. (2015). Human blindsight is mediated by an intact geniculo-extrastriate pathway. *Elife*, 4.

Alary, F., Duquette, M., Goldstein, R., Elaine Chapman, C., Voss, P., La Buissonnière-Ariza, V., and Lepore, F. (2009). Tactile acuity in the blind: a closer look reveals superiority over the sighted in some but not all cutaneous tasks. *Neuropsychologia*, 47(10):2037–2043.

Alexander, D. C., Barker, G. J., and Arridge, S. R. (2002). Detection and modeling of non-gaussian apparent diffusion coefficient profiles in human brain data. *Magn. Reson. Med.*, 48(2):331–340.

Alexander, D. C., Hubbard, P. L., Hall, M. G., Moore, E. A., Ptito, M., Parker, G. J. M., and Dyrby, T. B. (2010). Orientationally invariant indices of axon diameter and density from diffusion MRI. *Neuroimage*, 52(4):1374–1389.

Allen, B., Spiegel, D. P., Thompson, B., Pestilli, F., and Rokers, B. (2015). Altered white matter in early visual pathways of humans with amblyopia. *Vision Res.*, 114:48–55.

Alvarez, I., Schwarzkopf, D. S., and Clark, C. A. (2015). Extrastriate projections in human optic radiation revealed by fMRI-informed tractography. *Brain Struct. Funct.*, 220(5):2519–2532.

Amano, K., Wandell, B. A., and Dumoulin, S. O. (2009). Visual field maps, population receptive field sizes, and visual field coverage in the human MT+ complex. *J. Neurophysiol.*, 102:2704–2718.

Andersson, J. L. R. and Sotiropoulos, S. N. (2016). An integrated approach to correction for off-resonance effects and subject movement in diffusion MR imaging. *Neuroimage*, 125:1063–1078.

Arcaro, M. J., McMains, S. A., Singer, B. D., and Kastner, S. (2009). Retinotopic organization of human ventral visual cortex. *J. Neurosci.*, 29:10638–10652.

Arcaro, M. J., Pinsk, M. A., and Kastner, S. (2015). The anatomical and functional organization of the human visual pulvinar. *J. Neurosci.*, 35(27):9848–9871.

Ashida, H., Lingnau, A., Wall, M. B., and Smith, A. T. (2007). FMRI adaptation reveals separate mechanisms for first-order and second-order motion. *J. Neurophysiol.*, 97(2):1319–1325.

Assaf, Y., Alexander, D. C., Jones, D. K., Bizzi, A., Behrens, T. E. J., Clark, C. A., Cohen, Y., Dyrby, T. B., Huppi, P. S., Knoesche, T. R., Lebihan, D., Parker, G. J. M., Poupon, C., CONNECT consortium, Anaby, D., Anwander, A., Bar, L., Barazany, D., Blumenfeld-Katzir, T., De-Santis, S., Duclap, D., Figini, M., Fischi, E., Guevara, P., Hubbard, P., Hofstetter, S., Jbabdi, S., Kunz, N., Lazeyras, F., Lebois, A., Liptrot, M. G., Lundell, H., Mangin, J.-F., Dominguez, D. M., Morozov, D., Schreiber, J., Seunarine, K., Nava, S., Poupon, C., Riffert, T., Sasson, E., Schmitt, B., Shemesh, N., Sotiropoulos, S. N., Tavor, I., Zhang, H. G., and Zhou, F.-L. (2013). The CONNECT project: Combining macro- and micro-structure. *Neuroimage*, 80:273–282.

Assaf, Y. and Basser, P. J. (2005). Composite hindered and restricted model of diffusion (CHARMED) MR imaging of the human brain. *Neuroimage*, 27(1):48–58.

Assaf, Y., Blumenfeld-Katzir, T., Yovel, Y., and Basser, P. J. (2008). AxCaliber: a method for measuring axon diameter distribution from diffusion MRI. *Magn. Reson. Med.*, 59(6):1347–1354.

Avidan, G., Hasson, U., Malach, R., and Behrmann, M. (2005). Detailed exploration of face-related processing in congenital prosopagnosia: 2. functional neuroimaging findings. *J. Cogn. Neurosci.*, 17(7):1150–1167.

Avidan, G., Tanzer, M., Hadj-Bouziane, F., Liu, N., Ungerleider, L. G., and Behrmann, M. (2014). Selective dissociation between core and extended regions of the face processing network in congenital prosopagnosia. *Cereb. Cortex*, 24(6):1565–1578.

Backus, B. T., Fleet, D. J., Parker, A. J., and Heeger, D. J. (2001). Human cortical activity correlates with stereoscopic depth perception. *J. Neurophysiol.*, 86(4):2054–2068.

Bar, M., Kassam, K. S., Ghuman, A. S., Boshyan, J., Schmid, A. M., Schmidt, A. M., Dale, A. M., Hämäläinen, M. S., Marinkovic, K., Schacter, D. L., Rosen, B. R., and Halgren, E. (2006). Top-down facilitation of visual recognition. *Proc. Natl. Acad. Sci. U. S. A.*, 103(2):449–454.

Basser, P. J., Mattiello, J., and LeBihan, D. (1994a). Estimation of the effective self-diffusion tensor from the NMR spin echo. *J. Magn. Reson. B*, 103(3):247–254.

Basser, P. J., Mattiello, J., and LeBihan, D. (1994b). MR diffusion tensor spectroscopy and imaging. *Biophys. J.*, 66(1):259–267.

Bastiani, M. and Roebroeck, A. (2015). Unraveling the multiscale structural organization and connectivity of the human brain: the role of diffusion MRI. *Front. Neuroanat.*, 9.

Beaulieu, C. (2002). The basis of anisotropic water diffusion in the nervous system – a technical review. *NMR Biomed.*, 15(7-8):435–455.

997 Beaulieu, C., Does, M. D., Snyder, R. E., and Allen, P. S. (1996). Changes in water diffusion due
998 to wallerian degeneration in peripheral nerve. *Magn. Reson. Med.*, 36(4):627–631.

999 Bedny, M., Pascual-Leone, A., Dodell-Feder, D., Fedorenko, E., and Saxe, R. (2011). Language
1000 processing in the occipital cortex of congenitally blind adults. *Proc. Natl. Acad. Sci. U. S. A.*,
1001 108(11):4429–4434.

1002 Behrens, T., Woolrich, M. W., Jenkinson, M., Johansen-Berg, H., Nunes, R. G., Clare, S.,
1003 Matthews, P. M., Brady, J. M., and Smith, S. M. (2003). Characterization and propagation of
1004 uncertainty in diffusion-weighted MR imaging. *Magn. Reson. Med.*, 50(5):1077–1088.

1005 Behrens, T. E. J., Berg, H. J., Jbabdi, S., Rushworth, M. F. S., and Woolrich, M. W. (2007). Prob-
1006 abilistic diffusion tractography with multiple fibre orientations: What can we gain? *Neuroimage*,
1007 34(1):144–155.

1008 Bengtsson, S. L., Nagy, Z., Skare, S., Forsman, L., Forssberg, H., and Ullén, F. (2005). Extensive
1009 piano practicing has regionally specific effects on white matter development. *Nat. Neurosci.*,
1010 8(9):1148–1150.

1011 Blumenfeld-Katzir, T., Pasternak, O., Dagan, M., and Assaf, Y. (2011). Diffusion MRI of structural
1012 brain plasticity induced by a learning and memory task. *PLoS One*, 6(6):e20678.

1013 Bock, A. S. and Fine, I. (2014). Anatomical and functional plasticity in early blind individuals and
1014 the mixture of experts architecture. *Front. Hum. Neurosci.*, 8:971.

1015 Bock, A. S., Saenz, M., Tungaraza, R., Boynton, G. M., Bridge, H., and Fine, I. (2013). Visual
1016 callosal topography in the absence of retinal input. *Neuroimage*, 81:325–334.

1017 Boutet, I. and Faubert, J. (2006). Recognition of faces and complex objects in younger and older
1018 adults. *Mem. Cognit.*, 34(4):854–864.

1019 Brewer, A. A., Liu, J., Wade, A. R., and Wandell, B. A. (2005). Visual field maps and stimulus
1020 selectivity in human ventral occipital cortex. *Nat. Neurosci.*, 8:1102–1109.

1021 Bridge, H., Clare, S., and Krug, K. (2014). Delineating extrastriate visual area MT(V5) using
1022 cortical myeloarchitecture. *Neuroimage*, 93 Pt 2:231–236.

1023 Bridge, H., Cowey, A., Ragge, N., and Watkins, K. (2009). Imaging studies in congenital anoph-
1024 thalmia reveal preservation of brain architecture in 'visual' cortex. *Brain*, 132(Pt 12):3467–3480.

1025 Bridge, H., Hicks, S. L., Xie, J., Okell, T. W., Mannan, S., Alexander, I., Cowey, A., and Kennard,
1026 C. (2010). Visual activation of extra-striate cortex in the absence of V1 activation. *Neuropsy-*
1027 *chologia*, 48(14):4148–4154.

1028 Bridge, H., Thomas, O., Jbabdi, S., and Cowey, A. (2008). Changes in connectivity after visual
1029 cortical brain damage underlie altered visual function. *Brain*, 131(Pt 6):1433–1444.

1030 Bullock, T. H., Bennett, M. V. L., Johnston, D., Josephson, R., Marder, E., and Fields, R. D. (2005).
1031 Neuroscience. the neuron doctrine, redux. *Science*, 310(5749):791–793.

1032 Burton, H., Diamond, J. B., and McDermott, K. B. (2003). Dissociating cortical regions activated
1033 by semantic and phonological tasks: a FMRI study in blind and sighted people. *J. Neurophysiol.*,
1034 90(3):1965–1982.

1035 Caiafa, C. F. and Pestilli, F. (2015). Sparse multiway decomposition for analysis and modeling of
1036 diffusion imaging and tractography.

1037 Catani, M., Bodi, I., and Dell'Acqua, F. (2012). Comment on "the geometric structure of the brain
1038 fiber pathways". *Science*, 337(6102):1605.

1039 Catani, M., Howard, R. J., Pajevic, S., and Jones, D. K. (2002). Virtual in vivo interactive dissection
1040 of white matter fasciculi in the human brain. *Neuroimage*, 17(1):77–94.

1041 Catani, M., Jones, D. K., Donato, R., and Ffytche, D. H. (2003). Occipito-temporal connections in
1042 the human brain. *Brain*, 126(Pt 9):2093–2107.

1043 Catani, M. and Thiebaut de Schotten, M. (2008). A diffusion tensor imaging tractography atlas for
1044 virtual in vivo dissections. *Cortex*, 44(8):1105–1132.

1045 Clark, C. A. and Le Bihan, D. (2000). Water diffusion compartmentation and anisotropy at high b
1046 values in the human brain. *Magn. Reson. Med.*, 44(6):852–859.

1047 Cohen, L. G., Celnik, P., Pascual-Leone, A., Corwell, B., Falz, L., Dambrosia, J., Honda, M.,
1048 Sadato, N., Gerloff, C., Catalá, M. D., and Hallett, M. (1997). Functional relevance of cross-
1049 modal plasticity in blind humans. *Nature*, 389(6647):180–183.

1050 Conturo, T. E., Lori, N. F., Cull, T. S., Akbudak, E., Snyder, A. Z., Shimony, J. S., McKinstry, R. C.,
1051 Burton, H., and Raichle, M. E. (1999). Tracking neuronal fiber pathways in the living human
1052 brain. *Proc. Natl. Acad. Sci. U. S. A.*, 96(18):10422–10427.

1053 Cook, P. A., Bai, Y., Nedjati-Gilani, S., Seunarine, K. K., Hall, M. G., Parker, G. J., and Alexan-
1054 der, D. C. (2006). Camino: open-source diffusion-MRI reconstruction and processing. In *14th*
1055 *scientific meeting of the international society for magnetic resonance in medicine*, volume 2759.

1056 Côté, M.-A., Girard, G., Boré, A., Garyfallidis, E., Houde, J.-C., and Descoteaux, M. (2013). Trac-
1057 tometer: towards validation of tractography pipelines. *Med. Image Anal.*, 17(7):844–857.

1058 Cottereau, B. R., McKee, S. P., Ales, J. M., and Norcia, A. M. (2011). Disparity-tuned population
1059 responses from human visual cortex. *J. Neurosci.*, 31(3):954–965.

1060 Coullon, G. S. L., Emir, U. E., Fine, I., Watkins, K. E., and Bridge, H. (2015). Neurochemical
1061 changes in the pericalcarine cortex in congenital blindness attributable to bilateral anophthalmia.
1062 *J. Neurophysiol.*, 114(3):1725–1733.

1063 Crosby, E. C. (1962). *Correlative anatomy of the nervous system*. Macmillan.

1064 Daducci, A., Alessandro, D., Palu, A. D., Alia, L., and Jean-Philippe, T. (2015). COMMIT: Convex
1065 optimization modeling for microstructure informed tractography. *IEEE Trans. Med. Imaging*,
1066 34(1):246–257.

1067 Daducci, A., Dal Palú, A., Descoteaux, M., and Thiran, J.-P. (2016). Microstructure informed
1068 tractography: Pitfalls and open challenges. *Front. Neurosci.*, 10:247.

1069 De Volder, A. G., Bol, A., Blin, J., Robert, A., Arno, P., Grandin, C., Michel, C., and Veraart, C.
1070 (1997). Brain energy metabolism in early blind subjects: neural activity in the visual cortex.
1071 *Brain Res.*, 750(1-2):235–244.

1072 Deacon, T. (1989). Holism and associationism in neuropsychology: An anatomical synthesis.
1073 *Integrating theory and practice in clinical neuropsychology*, pages 1–47.

1074 Dehay, C., Giroud, P., Berland, M., Killackey, H. P., and Kennedy, H. (1996). Phenotypic character-
1075 isation of respecified visual cortex subsequent to prenatal enucleation in the monkey: develop-
1076 ment of acetylcholinesterase and cytochrome oxidase patterns. *J. Comp. Neurol.*, 376(3):386–
1077 402.

1078 Déjerine, J. (1895). *Anatomie des centres nerveux*, volume 1. Rueff et Cie., Paris.

1079 Dell'Acqua, F., Rizzo, G., Scifo, P., Clarke, R. A., Scotti, G., and Fazio, F. (2007). A model-based
1080 deconvolution approach to solve fiber crossing in diffusion-weighted MR imaging. *IEEE Trans.*
1081 *Biomed. Eng.*, 54(3):462–472.

1082 DeYoe, E. A., Bandettini, P., Neitz, J., Miller, D., and Winans, P. (1994). Functional magnetic
1083 resonance imaging (FMRI) of the human brain. *J. Neurosci. Methods*, 54:171–187.

1084 Dietrich, S., Hertrich, I., Kumar, V., and Ackermann, H. (2015). Experience-related structural
1085 changes of degenerated occipital white matter in late-blind humans - a diffusion tensor imaging
1086 study. *PLoS One*, 10(4):e0122863.

1087 Donoho, D. L. (2010). An invitation to reproducible computational research. *Biostatistics*,
1088 11(3):385–388.

1089 Dougherty, R. F., Ben-Shachar, M., Bammer, R., Brewer, A. A., and Wandell, B. A. (2005). Func-
1090 tional organization of human occipital-callosal fiber tracts. *Proc. Natl. Acad. Sci. U. S. A.*,
1091 102:7350–7355.

1092 Dougherty, R. F., Ben-Shachar, M., Deutsch, G. K., Hernandez, A., Fox, G. R., and Wandell, B. A.
1093 (2007). Temporal-callosal pathway diffusivity predicts phonological skills in children. *Proc. Natl.*
1094 *Acad. Sci. U. S. A.*, 104:8556–8561.

1095 Duan, Y., Norcia, A. M., Yeatman, J. D., and Mezer, A. (2015). The structural properties of major
1096 white matter tracts in strabismic AmblyopiaMajor white matter tracts in strabismic amblyopia.
1097 *Invest. Ophthalmol. Vis. Sci.*, 56(9):5152–5160.

1098 Dubner, R. and Zeki, S. M. (1971). Response properties and receptive fields of cells in an anatom-
1099 ically defined region of the superior temporal sulcus in the monkey. *Brain Res.*, 35(2):528–532.

1100 Dumoulin, S. O. and Wandell, B. A. (2008). Population receptive field estimates in human visual
1101 cortex. *Neuroimage*, 39:647–660.

1102 Engel, S. A., Rumelhart, D. E., Wandell, B. A., Lee, A. T., Glover, G. H., Chichilnisky, E. J., and
1103 Shadlen, M. N. (1994). fMRI of human visual cortex. *Nature*, 369:525.

1104 Fang, F. and He, S. (2005). Cortical responses to invisible objects in the human dorsal and ventral
1105 pathways. *Nat. Neurosci.*, 8:1380–1385.

1106 Feinberg, D. A., Moeller, S., Smith, S. M., Auerbach, E., Ramanna, S., Gunther, M., Glasser, M. F.,
1107 Miller, K. L., Ugurbil, K., and Yacoub, E. (2010). Multiplexed echo planar imaging for sub-second
1108 whole brain FMRI and fast diffusion imaging. *PLoS One*, 5(12):e15710.

1109 Felleman, D. J. and Van Essen, D. C. (1991). Distributed hierarchical processing in the primate
1110 cerebral cortex. *Cereb. Cortex*, 1(1):1–47.

Ferizi, U., Scherrer, B., Schneider, T., Alipoor, M., Eufracio, O., Fick, R. H. J., Deriche, R., Nilsson, M., Loya-Olivas, A. K., Rivera, M., Poot, D. H. J., Ramirez-Manzanares, A., Marroquin, J. L., Rokem, A., Pötter, C., Dougherty, R. F., Sakaie, K., Wheeler-Kingshott, C., Warfield, S. K., Witzel, T., Wald, L. L., Raya, J. G., and Alexander, D. C. (2016). Diffusion MRI microstructure models with in vivo human brain connectom data: results from a multi-group comparison.

Ffytche, D. H., Guy, C. N., and Zeki, S. (1996). Motion specific responses from a blind hemifield. *Brain*, 119 (Pt 6):1971–1982.

Fick, R. H. J., Wassermann, D., Caruyer, E., and Deriche, R. (2016). MAPL: Tissue microstructure estimation using laplacian-regularized MAP-MRI and its application to HCP data. *Neuroimage*, 134:365–385.

Fields, R. D. (2004). The other half of the brain. *Sci. Am.*, 290(4):54–61.

Fields, R. D. (2008a). White matter in learning, cognition and psychiatric disorders. *Trends Neurosci.*, 31(7):361–370.

Fields, R. D. (2008b). White matter matters. *Sci. Am.*, 298(3):42–49.

Fields, R. D. (2013). Neuroscience: Map the other brain. *Nature*, 501(7465):25–27.

Fischer, E., Bulthoff, H. H., Logothetis, N. K., and Bartels, A. (2012). Human areas V3A and V6 compensate for self-induced planar visual motion. *Neuron*, 73:1228–1240.

Fischl, B. (2012). FreeSurfer. *Neuroimage*, 62(2):774–781.

Fox, C. J., Iaria, G., and Barton, J. J. S. (2008). Disconnection in prosopagnosia and face processing. *Cortex*, 44(8):996–1009.

Frank, L. R. (2001). Anisotropy in high angular resolution diffusion-weighted MRI. *Magn. Reson. Med.*, 45(6):935–939.

Frank, L. R. (2002). Characterization of anisotropy in high angular resolution diffusion-weighted MRI. *Magn. Reson. Med.*, 47(6):1083–1099.

Freeman, J. (2015). Open source tools for large-scale neuroscience. *Curr. Opin. Neurobiol.*, 32:156–163.

Garyfallidis, E., Brett, M., Amirbekian, B., Rokem, A., van der Walt, S., Descoteaux, M., Nimmo-Smith, I., and Dipy Contributors (2014). Dipy, a library for the analysis of diffusion MRI data. *Front. Neuroinform.*, 8:8.

Garyfallidis, E., Brett, M., Correia, M. M., Williams, G. B., and Nimmo-Smith, I. (2012). QuickBundles, a method for tractography simplification. *Front. Neurosci.*, 6:175.

Garyfallidis, E., Ocegueda, O., Wassermann, D., and Descoteaux, M. (2015). Robust and efficient linear registration of white-matter fascicles in the space of streamlines. *Neuroimage*, 117:124–140.

Genç, E., Bergmann, J., Tong, F., Blake, R., Singer, W., and Kohler, A. (2011). Callosal connections of primary visual cortex predict the spatial spreading of binocular rivalry across the visual hemifields. *Front. Hum. Neurosci.*, 5:161.

1148 Geschwind, N. (1965). Disconnexion syndromes in animals and man. *Brain*, 88(2):237–237.

1149 Gloor, P. (1997). *The temporal lobe and limbic system*. Oxford University Press, USA.

1150 Gobbini, M. I. and Haxby, J. V. (2007). Neural systems for recognition of familiar faces. *Neuropsy-*
1151 *chologia*, 45(1):32–41.

1152 Goga, C. and Türe, U. (2015). The anatomy of meyer's loop revisited: changing the anatomical
1153 paradigm of the temporal loop based on evidence from fiber microdissection. *J. Neurosurg.*,
1154 122(6):1253–1262.

1155 Goldreich, D. and Kanics, I. M. (2003). Tactile acuity is enhanced in blindness. *J. Neurosci.*,
1156 23(8):3439–3445.

1157 Gomez, J., Pestilli, F., Witthoft, N., Golarai, G., Liberman, A., Poltoratski, S., Yoon, J., and Grill-
1158 Spector, K. (2015). Functionally defined white matter reveals segregated pathways in human
1159 ventral temporal cortex associated with category-specific processing. *Neuron*, 85(1):216–227.

1160 Goncalves, N. R., Ban, H., Sanchez-Panchuelo, R. M., Francis, S. T., Schluppeck, D., and Welch-
1161 man, A. E. (2015). 7 tesla FMRI reveals systematic functional organization for binocular disparity
1162 in dorsal visual cortex. *J. Neurosci.*, 35:3056–3072.

1163 Gorgolewski, K. J. and Poldrack, R. (2016). A practical guide for improving transparency and
1164 reproducibility in neuroimaging research.

1165 Gougoux, F., Lepore, F., Lassonde, M., Voss, P., Zatorre, R. J., and Belin, P. (2004). Neuropsy-
1166 chology: pitch discrimination in the early blind. *Nature*, 430(6997):309.

1167 Green, D. M. and Swets, J. A. (1966). *Signal Detection Theory and Psychophysics*.

1168 Greenberg, A. S., Verstynen, T., Chiu, Y. C., Yantis, S., Schneider, W., and Behrmann, M. (2012).
1169 Visuotopic cortical connectivity underlying attention revealed with white-matter tractography. *J.*
1170 *Neurosci.*, 32:2773–2782.

1171 Grill-Spector, K., Kushnir, T., Edelman, S., Itzchak, Y., and Malach, R. (1998). Cue-invariant
1172 activation in object-related areas of the human occipital lobe. *Neuron*, 21:191–202.

1173 Grill-Spector, K., Kushnir, T., Hendler, T., and Malach, R. (2000). The dynamics of object-selective
1174 activation correlate with recognition performance in humans. *Nat. Neurosci.*, 3:837–843.

1175 Grossi, D., Soricelli, A., Ponari, M., Salvatore, E., Quarantelli, M., Prinster, A., and Trojano, L.
1176 (2014). Structural connectivity in a single case of progressive prosopagnosia: the role of the
1177 right inferior longitudinal fasciculus. *Cortex*, 56:111–120.

1178 Gschwind, M., Pourtois, G., Schwartz, S., Van De Ville, D., and Vuilleumier, P. (2012). White-matter
1179 connectivity between face-responsive regions in the human brain. *Cereb. Cortex*, 22(7):1564–
1180 1576.

1181 Hara, Y., Pestilli, F., and Gardner, J. L. (2014). Differing effects of attention in single-units and pop-
1182 ulations are well predicted by heterogeneous tuning and the normalization model of attention.
1183 *Front. Comput. Neurosci.*, 8:12.

1184 Hartline, D. K. and Colman, D. R. (2007). Rapid conduction and the evolution of giant axons and
1185 myelinated fibers. *Curr. Biol.*, 17(1):R29–35.

1186 Henschen, S. E. (1893). On the visual path and centre. *Brain*, 16(1-2):170–180.

1187 Hofstetter, S., Tavor, I., Moryosef, S. T., and Assaf, Y. (2013). Short-term learning induces white
1188 matter plasticity in the fornix. *J. Neurosci.*, 33(31):12844–12850.

1189 Holmes, G. and Lister, W. T. (1916). Disturbances of vision from cerebral lesions with special
1190 reference to the cortical representation of the macula. *Brain*, 39(1-2):34–73.

1191 Huk, A. C. and Heeger, D. J. (2002). Pattern-motion responses in human visual cortex. *Nat.*
1192 *Neurosci.*, 5(1):72–75.

1193 Innocenti, G. M. and Price, D. J. (2005). Exuberance in the development of cortical networks. *Nat.*
1194 *Rev. Neurosci.*, 6(12):955–965.

1195 Inouye, T. (1909). *Die Sehstroungen bei Schussverietzungen der kortikalen Sehsphare*. W. En-
1196 gelmann, Leipzig, Germany.

1197 James, T. W., Humphrey, G. K., Gati, J. S., Menon, R. S., and Goodale, M. A. (2002). Differential
1198 effects of viewpoint on object-driven activation in dorsal and ventral streams. *Neuron*, 35:793–
1199 801.

1200 Jbabdi, S., Saad, J., Sotiropoulos, S. N., Haber, S. N., Van Essen, D. C., and Behrens, T. E. (2015).
1201 Measuring macroscopic brain connections in vivo. *Nat. Neurosci.*, 18(11):1546–1555.

1202 Jelescu, I. O., Veraart, J., Fieremans, E., and Novikov, D. S. (2016). Degeneracy in model parame-
1203 ter estimation for multi-compartmental diffusion in neuronal tissue. *NMR Biomed.*, 29(1):33–47.

1204 Jensen, J. H. and Helpern, J. A. (2010). MRI quantification of non-gaussian water diffusion by
1205 kurtosis analysis. *NMR Biomed.*, 23(7):698–710.

1206 Jensen, J. H., Helpern, J. A., Ramani, A., Lu, H., and Kaczynski, K. (2005). Diffusional kurtosis
1207 imaging: the quantification of non-gaussian water diffusion by means of magnetic resonance
1208 imaging. *Magn. Reson. Med.*, 53(6):1432–1440.

1209 Jeurissen, B., Leemans, A., Tournier, J.-D., Jones, D. K., and Sijbers, J. (2013). Investigating
1210 the prevalence of complex fiber configurations in white matter tissue with diffusion magnetic
1211 resonance imaging. *Hum. Brain Mapp.*, 34(11):2747–2766.

1212 Jiang, F., Stecker, G. C., and Fine, I. (2014). Auditory motion processing after early blindness. *J.*
1213 *Vis.*, 14(13):4.

1214 Johansen-Berg, H. and Behrens, T. E. J. (2009). *Diffusion MRI*. Academic Press.

1215 Jones, D. K. (2004). The effect of gradient sampling schemes on measures derived from diffusion
1216 tensor MRI: A monte carlo study. *Magn. Reson. Med.*, 51(4):807–815.

1217 Jones, D. K., Knösche, T. R., and Turner, R. (2013). White matter integrity, fiber count, and other
1218 fallacies: the do's and don'ts of diffusion MRI. *Neuroimage*, 73:239–254.

1219 Kammen, A., Law, M., Tjan, B. S., Toga, A. W., and Shi, Y. (2015). Automated retinofugal vi-
1220 sual pathway reconstruction with multi-shell HARDI and FOD-based analysis. *Neuroimage*,
1221 125:767–779.

Kim, J. H., Renden, R., and von Gersdorff, H. (2013). Dysmyelination of auditory afferent axons increases the jitter of action potential timing during high-frequency firing. *J. Neurosci.*, 33(22):9402–9407.

Kim, M., Ducros, M., Carlson, T., Ronen, I., He, S., Ugurbil, K., and Kim, D.-S. (2006). Anatomical correlates of the functional organization in the human occipitotemporal cortex. *Magn. Reson. Imaging*, 24(5):583–590.

Kolster, H., Janssens, T., Orban, G. A., and Vanduffel, W. (2014). The retinotopic organization of macaque occipitotemporal cortex anterior to V4 and caudoventral to the middle temporal (MT) cluster. *J. Neurosci.*, 34(31):10168–10191.

Kolster, H., Mandeville, J. B., Arsenault, J. T., Ekstrom, L. B., Wald, L. L., and Vanduffel, W. (2009). Visual field map clusters in macaque extrastriate visual cortex. *J. Neurosci.*, 29(21):7031–7039.

Konen, C. S. and Kastner, S. (2008). Two hierarchically organized neural systems for object information in human visual cortex. *Nat. Neurosci.*, 11:224–231.

Larsson, J. and Heeger, D. J. (2006). Two retinotopic visual areas in human lateral occipital cortex. *J. Neurosci.*, 26:13128–13142.

Lashley, K. S. (1963). *Brain mechanisms and learning*. New York: Dover.

Le Bihan, D. and Iima, M. (2015). Diffusion magnetic resonance imaging: What water tells us about biological tissues. *PLoS Biol.*, 13(7):e1002203.

Lebel, C. and Beaulieu, C. (2011). Longitudinal development of human brain wiring continues from childhood into adulthood. *J. Neurosci.*, 31(30):10937–10947.

Lebel, C., Gee, M., Camicioli, R., Wieler, M., Martin, W., and Beaulieu, C. (2012). Diffusion tensor imaging of white matter tract evolution over the lifespan. *Neuroimage*, 60(1):340–352.

Leh, S. E., Johansen-Berg, H., and Ptito, A. (2006). Unconscious vision: new insights into the neuronal correlate of blindsight using diffusion tractography. *Brain*, 129(Pt 7):1822–1832.

Leong, J. K., Pestilli, F., Wu, C. C., Samanez-Larkin, G. R., and Knutson, B. (2016). White-Matter tract connecting anterior insula to nucleus accumbens correlates with reduced preference for positively skewed gambles. *Neuron*, 89(1):63–69.

Leporé, N., Voss, P., Lepore, F., Chou, Y.-Y., Fortin, M., Gougoux, F., Lee, A. D., Brun, C., Lassonde, M., Madsen, S. K., Toga, A. W., and Thompson, P. M. (2010). Brain structure changes visualized in early- and late-onset blind subjects. *Neuroimage*, 49(1):134–140.

Lessard, N., Paré, M., Lepore, F., and Lassonde, M. (1998). Early-blind human subjects localize sound sources better than sighted subjects. *Nature*, 395(6699):278–280.

Leuze, C. W. U., Anwander, A., Bazin, P.-L., Dhital, B., Stüber, C., Reimann, K., Geyer, S., and Turner, R. (2014). Layer-specific intracortical connectivity revealed with diffusion MRI. *Cereb. Cortex*, 24(2):328–339.

Lewis, L. B. and Fine, I. (2011). The effects of visual deprivation after infancy. In *Adler's Physiology of the Eye*, pages 750–766. Elsevier.

Mangin, J.-F., Fillard, P., Cointepas, Y., Le Bihan, D., Frouin, V., and Poupon, C. (2013). Toward global tractography. *Neuroimage*, 80:290–296.

Martino, J. and Garcia-Porrero, J. A. (2013). In reply: Wernicke's perpendicular fasciculus and vertical portion of the superior longitudinal fasciculus. *Neurosurgery*.

Maunsell, J. H. and Gibson, J. R. (1992). Visual response latencies in striate cortex of the macaque monkey. *J. Neurophysiol.*, 68(4):1332–1344.

McNutt, M. (2014). Reproducibility. *Science*, 343(6168):229–229.

Melbourne, A., Toussaint, N., Owen, D., Simpson, I., Anthopoulos, T., De Vita, E., Atkinson, D., and Ourselin, S. (2016). NiftyFit: a software package for multi-parametric Model-Fitting of 4D magnetic resonance imaging data. *Neuroinformatics*.

Mezer, A., Yeatman, J. D., Stikov, N., Kay, K. N., Cho, N.-J., Dougherty, R. F., Perry, M. L., Parvizi, J., Hua, L. H., Butts-Pauly, K., and Wandell, B. A. (2013). Quantifying the local tissue volume and composition in individual brains with magnetic resonance imaging. *Nat. Med.*, 19(12):1667–1672.

Millman, J. K. and Brett, M. (2007). Analysis of functional magnetic resonance imaging in python. *Comput. Sci. Eng.*, 9(3):52–55.

Milner, A. D. and Goodale, M. A. (1995). *The visual brain in action*, volume 27. England.

Mohammadi, S., Carey, D., Dick, F., Diedrichsen, J., Sereno, M. I., Reisert, M., Callaghan, M. F., and Weiskopf, N. (2015). Whole-Brain in-vivo measurements of the axonal G-Ratio in a group of 37 healthy volunteers. *Front. Neurosci.*, 9.

Mori, S., Crain, B. J., Chacko, V. P., and van Zijl, P. C. (1999). Three-dimensional tracking of axonal projections in the brain by magnetic resonance imaging. *Ann. Neurol.*, 45(2):265–269.

Mori, S. and Van Zijl, P. C. M. (2002). Fiber tracking: principles and strategies-a technical review. *NMR Biomed.*, 15(7-8):468–480.

Morland, A. B., Jones, S. R., Finlay, A. L., Deyzac, E., Lê, S., and Kemp, S. (1999). Visual perception of motion, luminance and colour in a human hemianope. *Brain*, 122 (Pt 6):1183–1198.

Movshon, J. A., Adelson, E. H., Gizzi, M. S., and Newsome, W. T. (1985). The analysis of moving visual patterns. *Pattern recognition mechanisms*, 54:117–151.

Movshon, J. A. and Van Sluyters, R. C. (1981). Visual neural development. *Annu. Rev. Psychol.*, 32:477–522.

Mukherjee, P. (2005). Diffusion tensor imaging and fiber tractography in acute stroke. *Neuroimaging Clin. N. Am.*, 15(3):655–65, xii.

Mulkern, R. V., Gudbjartsson, H., Westin, C. F., Zengingonul, H. P., Gartner, W., Guttmann, C. R., Robertson, R. L., Kyriakos, W., Schwartz, R., Holtzman, D., Jolesz, F. A., and Maier, S. E. (1999). Multi-component apparent diffusion coefficients in human brain. *NMR Biomed.*, 12(1):51–62.

Nishida, S., Sasaki, Y., Murakami, I., Watanabe, T., and Tootell, R. B. H. (2003). Neuroimaging of direction-selective mechanisms for second-order motion. *J. Neurophysiol.*, 90(5):3242–3254.

Nooner, K. B., Colcombe, S. J., Tobe, R. H., Mennes, M., Benedict, M. M., Moreno, A. L., Panek, L. J., Brown, S., Zavitz, S. T., Li, Q., Sikka, S., Gutman, D., Bangaru, S., Schlachter, R. T., Kamiel, S. M., Anwar, A. R., Hinz, C. M., Kaplan, M. S., Rachlin, A. B., Adelsberg, S., Cheung, B., Khanuja, R., Yan, C., Craddock, C. C., Calhoun, V., Courtney, W., King, M., Wood, D., Cox, C. L., Kelly, A. M. C., Di Martino, A., Petkova, E., Reiss, P. T., Duan, N., Thomsen, D., Biswal, B., Coffey, B., Hoptman, M. J., Javitt, D. C., Pomara, N., Sidtis, J. J., Koplewicz, H. S., Castellanos, F. X., Leventhal, B. L., and Milham, M. P. (2012). The NKI-Rockland sample: A model for accelerating the pace of discovery science in psychiatry. *Front. Neurosci.*, 6:152.

Noppeney, U., Friston, K. J., Ashburner, J., Frackowiak, R., and Price, C. J. (2005). Early visual deprivation induces structural plasticity in gray and white matter. *Curr. Biol.*, 15(13):R488–90.

Ochsner, K. N. and Kosslyn, S. M. (1999). The cognitive neuroscience approach. In Bly, B. M. and Rumelhart, D. E., editors, *Handbook of Perception and Cognition; Cognitive Science*, volume 10, pages 319–365. books.google.com.

Ogawa, S., Takemura, H., Horiguchi, H., Terao, M., Haji, T., Pestilli, F., Yeatman, J. D., Tsuneoka, H., Wandell, B. A., and Masuda, Y. (2014). White matter consequences of retinal receptor and ganglion cell damage. *Invest. Ophthalmol. Vis. Sci.*, 55(10):6976–6986.

Özarslan, E., Koay, C. G., and Basser, P. J. (2013). Simple harmonic oscillator based reconstruction and estimation for One-Dimensional q-space magnetic resonance (1D-SHORE). In *Excursions in Harmonic Analysis, Volume 2*, Applied and Numerical Harmonic Analysis, pages 373–399. Birkhäuser Boston.

Peltier, J., Travers, N., Destrieux, C., and Velut, S. (2006). Optic radiations: a microsurgical anatomical study. *J. Neurosurg.*, 105(2):294–300.

Perez, F., Granger, B. E., and Hunter, J. D. (2010). Python: An ecosystem for scientific computing. *Comput. Sci. Eng.*, 13(2):13–21.

Pestilli, F., Carrasco, M., Heeger, D. J., and Gardner, J. L. (2011). Attentional enhancement via selection and pooling of early sensory responses in human visual cortex. *Neuron*, 72(5):832–846.

Pestilli, F. and Franco, P. (2015). Test-retest measurements and digital validation for in vivo neuroscience. *Scientific Data*, 2:140057.

Pestilli, F., Franco, P., Yeatman, J. D., Ariel, R., Kay, K. N., and Wandell, B. A. (2014). Evaluation and statistical inference for human connectomes. *Nat. Methods*, 11(10):1058–1063.

Petersen, S. E. and Sporns, O. (2015). Brain networks and cognitive architectures. *Neuron*, 88(1):207–219.

Philippi, C. L., Mehta, S., Grabowski, T., Adolphs, R., and Rudrauf, D. (2009). Damage to association fiber tracts impairs recognition of the facial expression of emotion. *J. Neurosci.*, 29(48):15089–15099.

Pierpaoli, C. and Basser, P. J. (1996). Toward a quantitative assessment of diffusion anisotropy. *Magn. Reson. Med.*, 36(6):893–906.

Poppel, E., Held, R., and Frost, D. (1973). Leter: Residual visual function after brain wounds involving the central visual pathways in man. *Nature*, 243(5405):295–296.

Portegies, J. M., Fick, R. H. J., Sanguinetti, G. R., Meesters, S. P. L., Girard, G., and Duits, R. (2015). Improving fiber alignment in HARDI by combining contextual PDE flow with constrained spherical deconvolution. *PLoS One*, 10(10):e0138122.

Press, W. A., Brewer, A. A., Dougherty, R. F., Wade, A. R., and Wandell, B. A. (2001). Visual areas and spatial summation in human visual cortex. *Vision Res.*, 41:1321–1332.

Ptito, M., Schneider, F. C. G., Paulson, O. B., and Kupers, R. (2008). Alterations of the visual pathways in congenital blindness. *Exp. Brain Res.*, 187(1):41–49.

Reid, R. C. (2012). From functional architecture to functional connectomics. *Neuron*, 75(2):209–217.

Reisert, M., Mader, I., Anastasopoulos, C., Weigel, M., Schnell, S., and Kiselev, V. (2011). Global fiber reconstruction becomes practical. *Neuroimage*, 54(2):955–962.

Reislev, N. L., Kupers, R., Siebner, H. R., Ptito, M., and Dyrby, T. B. (2015). Blindness alters the microstructure of the ventral but not the dorsal visual stream. *Brain Struct. Funct.*

Restrepo, C. E., Manger, P. R., Spenger, C., and Innocenti, G. M. (2003). Immature cortex lesions alter retinotopic maps and interhemispheric connections. *Ann. Neurol.*, 54(1):51–65.

Reveley, C., Seth, A. K., Pierpaoli, C., Silva, A. C., Yu, D., Saunders, R. C., Leopold, D. A., and Ye, F. Q. (2015). Superficial white matter fiber systems impede detection of long-range cortical connections in diffusion MR tractography. *Proc. Natl. Acad. Sci. U. S. A.*, 112(21):E2820–8.

Robel, S. and Sontheimer, H. (2016). Glia as drivers of abnormal neuronal activity. *Nat. Neurosci.*, 19(1):28–33.

Röder, B., Stock, O., Bien, S., Neville, H., and Rösler, F. (2002). Speech processing activates visual cortex in congenitally blind humans. *Eur. J. Neurosci.*, 16(5):930–936.

Röder, B., Teder-Sälejärvi, W., Sterr, A., Rösler, F., Hillyard, S. A., and Neville, H. J. (1999). Improved auditory spatial tuning in blind humans. *Nature*, 400(6740):162–166.

Rokem, A., Yeatman, J. D., Pestilli, F., Kay, K. N., Mezer, A., van der Walt, S., and Wandell, B. A. (2015). Evaluating the accuracy of diffusion MRI models in white matter. *PLoS One*, 10(4):e0123272.

Rubinov, M., Kötter, R., Hagmann, P., and Sporns, O. (2009). Brain connectivity toolbox: a collection of complex network measurements and brain connectivity datasets. *Neuroimage*, 47:S169.

Rudrauf, D., David, O., Lachaux, J.-P., Kovach, C. K., Martinerie, J., Renault, B., and Damasio, A. (2008). Rapid interactions between the ventral visual stream and emotion-related structures rely on a two-pathway architecture. *J. Neurosci.*, 28(11):2793–2803.

Sachs, H. (1892). *Das hemisphärenmark des menschlichen grosshirns*. Verlag von georg thieme, Leipzig.

1372 Sadato, N., Pascual-Leone, A., Grafman, J., Ibañez, V., Deiber, M. P., Dold, G., and Hallett, M.
1373 (1996). Activation of the primary visual cortex by braille reading in blind subjects. *Nature*,
1374 380(6574):526–528.

1375 Saenz, M. and Fine, I. (2010). Topographic organization of V1 projections through the corpus
1376 callosum in humans. *Neuroimage*, 52:1224–1229.

1377 Sagi, Y., Tavor, I., Hofstetter, S., Tzur-Moryosef, S., Blumenfeld-Katzir, T., and Assaf, Y. (2012).
1378 Learning in the fast lane: new insights into neuroplasticity. *Neuron*, 73(6):1195–1203.

1379 Salthouse, T. A. (2004). What and when of cognitive aging. *Curr. Dir. Psychol. Sci.*, 13(4):140–144.

1380 Sampaio-Baptista, C., Khrapitchev, A. A., Foxley, S., Schlagheck, T., Scholz, J., Jbabdi, S.,
1381 DeLuca, G. C., Miller, K. L., Taylor, A., Thomas, N., Kleim, J., Sibson, N. R., Bannerman, D., and
1382 Johansen-Berg, H. (2013). Motor skill learning induces changes in white matter microstructure
1383 and myelination. *J. Neurosci.*, 33(50):19499–19503.

1384 Scherf, K. S., Thomas, C., Doyle, J., and Behrmann, M. (2014). Emerging Structure–Function
1385 relations in the developing face processing system. *Cereb. Cortex*, 24(11):2964–2980.

1386 Sereno, M. I., Dale, A. M., Reppas, J. B., Kwong, K. K., Belliveau, J. W., Brady, T. J., Rosen, B. R.,
1387 and Tootell, R. B. (1995). Borders of multiple visual areas in humans revealed by functional
1388 magnetic resonance imaging. *Science*, 268:889–893.

1389 Sereno, M. I., Lutti, A., Weiskopf, N., and Dick, F. (2013). Mapping the human cortical surface by
1390 combining quantitative t(1) with retinotopy. *Cereb. Cortex*, 23(9):2261–2268.

1391 Setsompop, K., Kimmlingen, R., Eberlein, E., Witzel, T., Cohen-Adad, J., McNab, J. A., Keil, B.,
1392 Tisdall, M. D., Hoecht, P., Dietz, P., Cauley, S. F., Tountcheva, V., Matschl, V., Lenz, V. H.,
1393 Heberlein, K., Potthast, A., Thein, H., Van Horn, J., Toga, A., Schmitt, F., Lehne, D., Rosen,
1394 B. R., Wedeen, V., and Wald, L. L. (2013). Pushing the limits of in vivo diffusion MRI for the
1395 human connectome project. *Neuroimage*, 80:220–233.

1396 Sherbondy, A. J., Dougherty, R. F., Ben-Shachar, M., Napel, S., and Wandell, B. A. (2008a).
1397 ConTrack: finding the most likely pathways between brain regions using diffusion tractography.
1398 *J. Vis.*, 8(9):15.1–16.

1399 Sherbondy, A. J., Dougherty, R. F., Napel, S., and Wandell, B. A. (2008b). Identifying the human
1400 optic radiation using diffusion imaging and fiber tractography. *J. Vis.*, 8(10):12.1–11.

1401 Shimony, J. S., Burton, H., Epstein, A. A., McLaren, D. G., Sun, S. W., and Snyder, A. Z. (2006).
1402 Diffusion tensor imaging reveals white matter reorganization in early blind humans. *Cereb.*
1403 *Cortex*, 16(11):1653–1661.

1404 Shu, N., Liu, Y., Li, J., Li, Y., Yu, C., and Jiang, T. (2009). Altered anatomical network in early
1405 blindness revealed by diffusion tensor tractography. *PLoS One*, 4(9):e7228.

1406 Silver, M. A. and Kastner, S. (2009). Topographic maps in human frontal and parietal cortex.
1407 *Trends Cogn. Sci.*, 13(11):488–495.

1408 Simmons, D. M. and Swanson, L. W. (2009). Comparing histological data from different brains:
1409 sources of error and strategies for minimizing them. *Brain Res. Rev.*, 60(2):349–367.

Smith, A. T., Greenlee, M. W., Singh, K. D., Kraemer, F. M., and Hennig, J. (1998). The processing of first- and second-order motion in human visual cortex assessed by functional magnetic resonance imaging (fMRI). *J. Neurosci.*, 18:3816–3830.

Smith, R. E., Tournier, J.-D., Calamante, F., and Connelly, A. (2012). Anatomically-constrained tractography: improved diffusion MRI streamlines tractography through effective use of anatomical information. *Neuroimage*, 62(3):1924–1938.

Smith, R. E., Tournier, J.-D., Calamante, F., and Connelly, A. (2015). The effects of SIFT on the reproducibility and biological accuracy of the structural connectome. *Neuroimage*, 104:253–265.

Smith, S. M., Jenkinson, M., Woolrich, M. W., Beckmann, C. F., Behrens, T. E. J., Johansen-Berg, H., Bannister, P. R., De Luca, M., Drobnjak, I., Flitney, D. E., Niazy, R. K., Saunders, J., Vickers, J., Zhang, Y., De Stefano, N., Brady, J. M., and Matthews, P. M. (2004). Advances in functional and structural MR image analysis and implementation as FSL. *Neuroimage*, 23 Suppl 1:S208–19.

Song, S., Garrido, L., Nagy, Z., Mohammadi, S., Steel, A., Driver, J., Dolan, R. J., Duchaine, B., and Furl, N. (2015). Local but not long-range microstructural differences of the ventral temporal cortex in developmental prosopagnosia. *Neuropsychologia*, 78:195–206.

Song, S.-K., Yoshino, J., Le, T. Q., Lin, S.-J., Sun, S.-W., Cross, A. H., and Armstrong, R. C. (2005). Demyelination increases radial diffusivity in corpus callosum of mouse brain. *Neuroimage*, 26(1):132–140.

Sotiropoulos, S. N., Jbabdi, S., Xu, J., Andersson, J. L., Moeller, S., Auerbach, E. J., Glasser, M. F., Hernandez, M., Sapiro, G., Jenkinson, M., Feinberg, D. A., Yacoub, E., Lenglet, C., Van Essen, D. C., Ugurbil, K., Behrens, T. E., and Consortium, W. U-Minn HCP (2013). Advances in diffusion MRI acquisition and processing in the human connectome project. *Neuroimage*, 80:125–143.

Sporns, O. (2013). Structure and function of complex brain networks. *Dialogues Clin. Neurosci.*, 15(3):247–262.

Sporns, O., Tononi, G., and Kötter, R. (2005). The human connectome: A structural description of the human brain. *PLoS Comput. Biol.*, 1(4):e42.

Stikov, N., Campbell, J. S. W., Stroh, T., Lavelée, M., Frey, S., Novek, J., Nuara, S., Ho, M.-K., Bedell, B. J., Dougherty, R. F., Leppert, I. R., Boudreau, M., Narayanan, S., Duval, T., Cohen-Adad, J., Picard, P.-A., Gasecka, A., Côté, D., and Pike, G. B. (2015). In vivo histology of the myelin g-ratio with magnetic resonance imaging. *Neuroimage*, 118:397–405.

Stikov, N., Perry, L. M., Mezer, A., Rykhlevskaia, E., Wandell, B. A., Pauly, J. M., and Dougherty, R. F. (2011). Bound pool fractions complement diffusion measures to describe white matter micro and macrostructure. *Neuroimage*, 54(2):1112–1121.

Stodden, V., Leisch, F., and Peng, R. D. (2014). *Implementing Reproducible Research*. CRC Press.

Stüber, C., Morawski, M., Schäfer, A., Labadie, C., Wähnert, M., Leuze, C., Streicher, M., Barapatre, N., Reimann, K., Geyer, S., Spemann, D., and Turner, R. (2014). Myelin and iron concentration in the human brain: a quantitative study of MRI contrast. *Neuroimage*, 93 Pt 1:95–106.

Takemura, H., Caiafa, C. F., Wandell, B. A., and Pestilli, F. (2016). Ensemble tractography. *PLoS Comput. Biol.*, 12(2):e1004692.

Takemura, H., Rokem, A., Winawer, J., Yeatman, J. D., Wandell, B. A., and Pestilli, F. (2015). A major human white matter pathway between dorsal and ventral visual cortex. *Cereb. Cortex*.

Tamietto, M., Pullens, P., de Gelder, B., Weiskrantz, L., and Goebel, R. (2012). Subcortical connections to human amygdala and changes following destruction of the visual cortex. *Curr. Biol.*, 22(15):1449–1455.

Thomas, C., Avidan, G., Humphreys, K., Jung, K.-J., Gao, F., and Behrmann, M. (2009). Reduced structural connectivity in ventral visual cortex in congenital prosopagnosia. *Nat. Neurosci.*, 12(1):29–31.

Thomas, C. and Baker, C. I. (2013). Teaching an adult brain new tricks: a critical review of evidence for training-dependent structural plasticity in humans. *Neuroimage*, 73:225–236.

Thomas, C., Moya, L., Avidan, G., Humphreys, K., Jung, K. J., Peterson, M. A., and Behrmann, M. (2008). Reduction in white matter connectivity, revealed by diffusion tensor imaging, may account for age-related changes in face perception. *J. Cogn. Neurosci.*, 20(2):268–284.

Thomas, C., Ye, F. Q., Irfanoglu, M. O., Modi, P., Saleem, K. S., Leopold, D. A., and Pierpaoli, C. (2014). Anatomical accuracy of brain connections derived from diffusion MRI tractography is inherently limited. *Proc. Natl. Acad. Sci. U. S. A.*, 111(46):16574–16579.

Thomason, M. E. and Thompson, P. M. (2011). Diffusion imaging, white matter, and psychopathology. *Annu. Rev. Clin. Psychol.*, 7:63–85.

Tomaiuolo, F., Campana, S., Collins, D. L., Fonov, V. S., Ricciardi, E., Sartori, G., Pietrini, P., Kupers, R., and Ptito, M. (2014). Morphometric changes of the corpus callosum in congenital blindness. *PLoS One*, 9(9):e107871.

Tootell, R. B., Mendola, J. D., Hadjikhani, N. K., Ledden, P. J., Liu, A. K., Reppas, J. B., Sereno, M. I., and Dale, A. M. (1997). Functional analysis of V3A and related areas in human visual cortex. *J. Neurosci.*, 17:7060–7078.

Tootell, R. B., Reppas, J. B., Kwong, K. K., Malach, R., Born, R. T., Brady, T. J., Rosen, B. R., and Belliveau, J. W. (1995). Functional analysis of human MT and related visual cortical areas using magnetic resonance imaging. *J. Neurosci.*, 15(4):3215–3230.

Tournier, J.-D., Calamante, F., and Connelly, A. (2007). Robust determination of the fibre orientation distribution in diffusion MRI: non-negativity constrained super-resolved spherical deconvolution. *Neuroimage*, 35(4):1459–1472.

Tournier, J.-D., Calamante, F., and Connelly, A. (2012). MRtrix: Diffusion tractography in crossing fiber regions. *Int. J. Imaging Syst. Technol.*, 22(1):53–66.

Tournier, J.-D., Calamante, F., Gadian, D. G., and Connelly, A. (2004). Direct estimation of the fiber orientation density function from diffusion-weighted MRI data using spherical deconvolution. *Neuroimage*, 23(3):1176–1185.

1486 Tsao, D. Y., Vanduffel, W., Sasaki, Y., Fize, D., Knutsen, T. A., Mandeville, J. B., Wald, L. L., Dale,
1487 A. M., Rosen, B. R., Van Essen, D. C., Livingstone, M. S., Orban, G. A., and Tootell, R. B.
1488 (2003). Stereopsis activates V3A and caudal intraparietal areas in macaques and humans.
1489 *Neuron*, 39:555–568.

1490 Tuch, D. S. (2004). Q-ball imaging. *Magn. Reson. Med.*, 52(6):1358–1372.

1491 Uhl, F., Franzen, P., Podreka, I., Steiner, M., and Deecke, L. (1993). Increased regional cerebral
1492 blood flow in inferior occipital cortex and cerebellum of early blind humans. *Neurosci. Lett.*,
1493 150(2):162–164.

1494 Ungerleider, L. G. and Haxby, J. V. (1994). 'what' and 'where' in the human brain. *Curr. Opin.*
1495 *Neurobiol.*, 4:157–165.

1496 Ungerleider, L. G. and Mishkin, M. (1982). Two cortical visual systems. In Ingle, D. J., Goodale,
1497 M. A., and Mansfield, R. J. W., editors, *The analysis of visual behavior.*, pages 549–586. MIT
1498 Press, Cambridge, MA.

1499 Van Boven, R. W., Hamilton, R. H., Kauffman, T., Keenan, J. P., and Pascual-Leone, A. (2000).
1500 Tactile spatial resolution in blind braille readers. *Neurology*, 54(12):2230–2236.

1501 Van Essen, D. C., Smith, S. M., Barch, D. M., Behrens, T. E. J., Yacoub, E., Ugurbil, K., and
1502 WU-Minn HCP Consortium (2013). The WU-Minn human connectome project: an overview.
1503 *Neuroimage*, 80:62–79.

1504 Vanduffel, W., Zhu, Q., and Orban, G. A. (2014). Monkey cortex through fMRI glasses. *Neuron*,
1505 83(3):533–550.

1506 Veenith, T. V., Carter, E., Grossac, J., Newcombe, V. F. J., Outtrim, J. G., Lupson, V., Williams,
1507 G. B., Menon, D. K., and Coles, J. P. (2013). Inter subject variability and reproducibility of diffu-
1508 sion tensor imaging within and between different imaging sessions. *PLoS One*, 8(6):e65941.

1509 Vidyasagar, T. R. and Pammer, K. (2010). Dyslexia: a deficit in visuo-spatial attention, not in
1510 phonological processing. *Trends Cogn. Sci.*, 14(2):57–63.

1511 Voss, P., Lassonde, M., Gougoux, F., Fortin, M., Guillemot, J.-P., and Lepore, F. (2004). Early-
1512 and late-onset blind individuals show supra-normal auditory abilities in far-space. *Curr. Biol.*,
1513 14(19):1734–1738.

1514 Vu, A. T., Auerbach, E., Lenglet, C., Moeller, S., Sotiropoulos, S. N., Jbabdi, S., Andersson, J.,
1515 Yacoub, E., and Ugurbil, K. (2015). High resolution whole brain diffusion imaging at 7T for the
1516 human connectome project. *Neuroimage*, 122:318–331.

1517 Wade, A. R., Brewer, A. A., Rieger, J. W., and Wandell, B. A. (2002). Functional measurements of
1518 human ventral occipital cortex: retinotopy and colour. *Philos. Trans. R. Soc. Lond. B Biol. Sci.*,
1519 357:963–973.

1520 Wakana, S., Caprihan, A., Panzenboeck, M. M., Fallon, J. H., Perry, M., Gollub, R. L., Hua, K.,
1521 Zhang, J., Jiang, H., Dubey, P., Blitz, A., van Zijl, P., and Mori, S. (2007). Reproducibility of
1522 quantitative tractography methods applied to cerebral white matter. *Neuroimage*, 36(3):630–
1523 644.

1524 Wandell, B. A. (2016). Clarifying human white matter. *Annu. Rev. Neurosci.*, 39(1).

Wandell, B. A., Dumoulin, S. O., and Brewer, A. A. (2007). Visual field maps in human cortex. *Neuron*, 56(2):366–383.

Wandell, B. A., Rokem, A., Perry, L. M., Schaefer, G., and Dougherty, R. F. (2015). Data management to support reproducible research.

Wandell, B. A. and Winawer, J. (2011). Imaging retinotopic maps in the human brain. *Vision Res.*, 51(7):718–737.

Wang, D., Qin, W., Liu, Y., Zhang, Y., Jiang, T., and Yu, C. (2013). Altered white matter integrity in the congenital and late blind people. *Neural Plast.*, 2013:128236.

Wassermann, D., Bloy, L., Kanterakis, E., Verma, R., and Deriche, R. (2010). Unsupervised white matter fiber clustering and tract probability map generation: applications of a gaussian process framework for white matter fibers. *Neuroimage*, 51(1):228–241.

Watkins, K. E., Cowey, A., Alexander, I., Filippini, N., Kennedy, J. M., Smith, S. M., Ragge, N., and Bridge, H. (2012). Language networks in anophthalmia: maintained hierarchy of processing in 'visual' cortex. *Brain*, 135(Pt 5):1566–1577.

Watson, J. D., Myers, R., Frackowiak, R. S., Hajnal, J. V., Woods, R. P., Mazziotta, J. C., Shipp, S., and Zeki, S. (1993). Area V5 of the human brain: evidence from a combined study using positron emission tomography and magnetic resonance imaging. *Cereb. Cortex*, 3(2):79–94.

Waxman, S. G. and Bennett, M. V. (1972). Relative conduction velocities of small myelinated and non-myelinated fibres in the central nervous system. *Nat. New Biol.*, 238(85):217–219.

Weaver, K. E., Richards, T. L., Saenz, M., Petropoulos, H., and Fine, I. (2013). Neurochemical changes within human early blind occipital cortex. *Neuroscience*, 252:222–233.

Webster, M. J., Ungerleider, L. G., and Bachevalier, J. (1991). Lesions of inferior temporal area TE in infant monkeys alter cortico-amygdalar projections. *Neuroreport*, 2(12):769–772.

Wedeen, V. J., Hagmann, P., Tseng, W.-Y. I., Reese, T. G., and Weisskoff, R. M. (2005). Mapping complex tissue architecture with diffusion spectrum magnetic resonance imaging. *Magn. Reson. Med.*, 54(6):1377–1386.

Wedeen, V. J., Rosene, D. L., Wang, R., Dai, G., Mortazavi, F., Hagmann, P., Kaas, J. H., and Tseng, W.-Y. I. (2012a). The geometric structure of the brain fiber pathways. *Science*, 335(6076):1628–1634.

Wedeen, V. J., Rosene, D. L., Wang, R., Dai, G., Mortazavi, F., Hagmann, P., Kaas, J. H., and Tseng, W.-Y. I. (2012b). Response to comment on "the geometric structure of the brain fiber pathways". *Science*, 337(6102):1605.

Weiner, K. S., Yeatman, J. D., and Wandell, B. A. (2016). The posterior arcuate fasciculus and the vertical occipital fasciculus. *Cortex*.

Weiskrantz, L., Warrington, E. K., Sanders, M. D., and Marshall, J. (1974). Visual capacity in the hemianopic field following a restricted occipital ablation. *Brain*, 97(4):709–728.

Wernicke, C. (1881). *Lehrbuch der Gehirnkrankheiten für Aerzte und Studirende*. Kassel Theodor Fischer.

Wiesel, T. N. and Hubel, D. H. (1963). Single-cell responses in striate cortex of kittens deprived of vision in one eye. *J. Neurophysiol.*, 26:1003–1017.

Wiesel, T. N. and Hubel, D. H. (1965a). Comparison of the effects of unilateral and bilateral eye closure on cortical unit responses in kittens. *J. Neurophysiol.*, 28(6):1029–1040.

Wiesel, T. N. and Hubel, D. H. (1965b). Extent of recovery from the effects of visual deprivation in kittens. *J. Neurophysiol.*, 28(6):1060–1072.

Wiesel, T. N., Hubel, D. H., and Others (1963). Effects of visual deprivation on morphology and physiology of cells in the cat's lateral geniculate body. *J. Neurophysiol.*, 26(978):6.

Winawer, J., Horiguchi, H., Sayres, R. A., Amano, K., and Wandell, B. A. (2010). Mapping hv4 and ventral occipital cortex: the venous eclipse. *J. Vis.*, 10:1.

Winawer, J. and Witthoft, N. (2015). Human V4 and ventral occipital retinotopic maps. *Vis. Neurosci.*, 32:E020.

Wolf, I., Vetter, M., Wegner, I., Böttger, T., Nolden, M., Schöbinger, M., Hastenteufel, M., Kunert, T., and Meinzer, H.-P. (2005). The medical imaging interaction toolkit. *Med. Image Anal.*, 9(6):594–604.

Xue, R., van Zijl, P., Crain, B. J., Solaiyappan, M., and Mori, S. (1999). In vivo three-dimensional reconstruction of rat brain axonal projections by diffusion tensor imaging. *Magn. Reson. Med.*, 42(6):1123–1127.

Yaffe, M. B. (2015). Reproducibility in science. *Sci. Signal.*, 8(371):eg5–eg5.

Yeatman, J. D., Dougherty, R. F., Myall, N. J., Wandell, B. A., and Feldman, H. M. (2012). Tract profiles of white matter properties: automating fiber-tract quantification. *PLoS One*, 7(11):e49790.

Yeatman, J. D., Dougherty, R. F., Rykhlevskaia, E., Sherbondy, A. J., Deutsch, G. K., Wandell, B. A., and Ben-Shachar, M. (2011). Anatomical properties of the arcuate fasciculus predict phonological and reading skills in children. *J. Cogn. Neurosci.*, 23(11):3304–3317.

Yeatman, J. D., Rauschecker, A. M., and Wandell, B. A. (2013). Anatomy of the visual word form area: adjacent cortical circuits and long-range white matter connections. *Brain Lang.*, 125:146–155.

Yeatman, J. D., Wandell, B. A., and Mezer, A. A. (2014a). Lifespan maturation and degeneration of human brain white matter. *Nat. Commun.*, 5:4932.

Yeatman, J. D., Weiner, K. S., Pestilli, F., Rokem, A., Mezer, A., and Wandell, B. A. (2014b). The vertical occipital fasciculus: a century of controversy resolved by in vivo measurements. *Proc. Natl. Acad. Sci. U. S. A.*, 111(48):E5214–23.

Yendiki, A., Panneck, P., Srinivasan, P., Stevens, A., Zöllei, L., Augustinack, J., Wang, R., Salat, D., Ehrlich, S., Behrens, T., Jbabdi, S., Gollub, R., and Fischl, B. (2011). Automated probabilistic reconstruction of white-matter pathways in health and disease using an atlas of the underlying anatomy. *Front. Neuroinform.*, 5:23.

Zhang, H., Awate, S. P., Das, S. R., Woo, J. H., Melhem, E. R., Gee, J. C., and Yushkevich, P. A. (2010). A tract-specific framework for white matter morphometry combining macroscopic and microscopic tract features. *Med. Image Anal.*, 14(5):666–673.

1602 Zhang, H., Schneider, T., Wheeler-Kingshott, C. A., and Alexander, D. C. (2012). NODDI: practical
1603 in vivo neurite orientation dispersion and density imaging of the human brain. *Neuroimage*,
1604 61:1000–1016.